UNIVERSITÀ DEGLI STUDI DI PALERMO
Dottorato di ricerca in Oncologia e Chirurgia Sperimentali
Dipartimento di Discipline Chirurgiche Oncologiche e Stomatologiche (Di.Chir.On.S.)

International joint PhD program - University of Palermo (Italy) and Universiteit Antwerpen (Belgium)

Exosomes analysis in Non Small Cell Lung Cancer: from *in vitro* models to preclinical application

Doctoral Dissertation of:
Dr. Marzia Pucci

Supervisors:

Prof. Alessandra Modesti
Prof. Umberto Malapelle

Tutor Unipa:
Prof. Riccardo Alessandro

Tutors UAntwerpen:
Prof. Dr. Marc Peeters
Prof. Dr. Christian Rolfo

The Chair of the Doctoral Program:
Prof. Giuseppina Campisi

Years 2015/2017-Cycle XXX

Faculty of Medicine and Health Sciences

Dipartimento di Discipline Chirurgiche Oncologiche e Stomatologiche (Di.Chir.On.S.)

International joint PhD program - University of Palermo (Italy) and Universiteit Antwerpen (Belgium)

Title of the thesis:

Exosomes analysis in Non Small Cell Lung Cancer: from *in vitro* models to preclinical application

Doctoral Dissertation of:
Dr. Marzia Pucci

Supervisors:
Prof. Alessandra Modesti
Prof. Umberto Malapelle

Tutor Unipa:
Prof. Riccardo Alessandro

Tutors UAntwerpen:
Prof. Dr. Marc Peeters
Prof. Dr. Christian Rolfo

The Chair of the Doctoral Program:
Prof. Giuseppina Campisi

Thesis for the Degree of Doctor in Medical Sciences (In de medische wetenschappen) at the Universiteit Antwerpen to be defended by Marzia Pucci.

Thesis for the Degree of Doctor in Experimental Oncology and Surgery – (University of Palermo).

INDEX

Abstract

Non-small cell lung cancer (NSCLC) remains the leading cause of cancer-related deaths worldwide. The majority of patients are diagnosed in advanced disease stage. Bone metastasis is the most frequent complication in NSCLC resulting in osteolytic lesions. The perfect balance between bone-resorbing osteoclasts and bone-forming osteoblasts activity is lost in bone metastasis, inducing osteoclastogenesis. In NSCLC, the epidermal growth factor receptor (EGFR) pathway is constitutively activated. EGFR binds Amphiregulin (AREG) that is overexpressed in several cancers such as colon, breast and lung. Its levels in plasma of NSCLC patients correlate with poor prognosis and AREG was recently found as a signaling molecule in exosomes derived from cancer cell lines. Exosomes have a key role in the cell-cell communication and they were recently indicated as important actors in metastatic niche preparation. In the present work, we hypothesize a role of AREG carried by exosomes derived from NSCLC in bone metastasis induction. We observed that NSCLC-exosomes, containing AREG, induce EGFR pathway activation in pre-osteoclasts that in turn causes an increased expression of RANKL. RANKL is able to induce the expression of proteolytic enzymes, well-known markers of osteoclastogenesis, triggering a vicious cycle in osteolytic bone metastasis.

Samenvatting

Niet-kleincellige longkanker (NSCLC) is nog steeds de hoofdoorzaak van kankergerelateerde overlijdens wereldwijd. Bij de meeste patiënten wordt deze ziekte in een vroeg stadium gediagnosticeerd. Botmetastase is de meest voorkomende complicatie bij NSCLC en leidt tot osteolytische letsels. Het perfecte evenwicht tussen de activiteit van botresorberende osteoclasten en die van botvormende osteoblasten wordt door botmetastase verstoord, hetgeen leidt tot osteoclastogenese (botafbraak). Bij NSCLC wordt de baan van de epidermale groeifactor-receptor (EGFR) constitutief geactiveerd. EGFR bindt Amphiregulin (AREG) dat overduidelijk aanwezig is in diverse kankers, bijv. in karteldarm-, borst- en longkanker. De aanwezigheidsniveaus van AREG in plasma van NSCLC-patiënten correleren met een gebrekkige prognose en onlangs werd AREG geïdentificeerd als een informatie overbrengende (signaal)stof in exosomen afgeleid uit kankercellijnen. Exosomen spelen een belangrijke rol in de communicatie tussen cellen en zijn sinds kort ook geïdentificeerd als belangrijke actoren om de metastatische niche voor te bereiden. In dit werk veronderstellen wij dat AREG gedragen door exosomen afgeleid van NSCLC een rol spelen in het veroorzaken van botmetastase. Wij hebben opgemerkt dat NSCLC-exosomen die AREG bevatten een activering van de EGFR-baan in pre-osteoclasten teweegbrengen hetgeen op zijn beurt leidt tot een sterkere expressie van RANKL (receptor-activator van nucleaire factor kappa-B-ligand). RANKL kan leiden tot de expressie van proteolytische enzymen, goed gekende merkers van botafbraak, die een vicieuze cyclus op gang brengen in osteolytische botmetastase.

Summary-Informative abstract

Introduction: Lung cancer represents the main cause of world cancer-related deaths. Malignant lung tumors can be subdivided into small-cell-lung carcinoma (SCLC) and non-SCLC (NSCLC). The three main subtypes of NSCLC are: squamous cell carcinoma, adenocarcinoma and large lung cell carcinoma. Almost 85% of lung cancers are classified as NSCLC and adenocarcinoma is the most frequent. The lack of clinical manifestations during the initial stages of lung cancer development, the absence of appropriate diagnostic, prognostic and predictive biomarkers and the limited efficacy of the available treatments correlate to high mortality rate. Bone metastasis is the most frequent complication in NSCLC resulting in osteolytic lesions. Bone microenvironment can promote the growth of lung cancer osteolytic metastases through the interaction of metastatic cells with osteoclasts and osteoblasts, inducing loss of the perfect balance between bone-resorbing and bone-forming cells activity. Several reports indicate that EGFR signaling is upregulated in NSCLC and in a variety of tumors metastasizing to the bone. Furthermore, it was demonstrated that EGFR regulates osteoclast differentiation through the crosstalk with RANK signaling. EGFR is bound and activated by a family of seven peptide growth factors among which we focused on Amphiregulin. This protein is overexpressed in several cancers such as colon, breast and lung. Its levels in plasma of NSCLC patients correlate with poor prognosis and AREG was recently found as a signaling molecule in exosomes derived from cancer cell lines. It has been described that exosomes have a key role in cell-cell communication and they were recently indicated as important actors in metastatic niche preparation. Recently our research group showed that multiple myeloma cells (MM) exosomes had a role in osteoclast differentiation. Raimondi et al., showed that exosomes released by MM cells are involved in osteoclasts differentiation. These exosomes induced the differentiation of murine macrophages (RAW 264.7) and human primary preosteoclasts in osteoclasts, increasing the expression of osteoclast markers such as Cathepsin K (CTSK), Matrix

Metalloproteinase 9 (MMP9), and Tartrate-resistant Acid Phosphatase (TRAP). **Results:** In the present work, we hypothesize a role of AREG carried by exosomes from NSCLC cells in bone metastasis induction. In order to demonstrate that AREG contained in NSCLC-exosomes plays a key role in the induction of pre-osteoclast differentiation in mature osteoclasts, exosomes isolated *in vitro* from CRL-2868 conditioned media and *in vivo* from plasma of NSCLC patients were characterized through morphological and biochemical analyses. In line with data from literature, we showed that RAW 264.7 cells treated with NSCLC exosomes activate the EGFR pathway that caused an upregulation of RANKL and of osteoclastogenesis markers (MMP9 and TRAP). In order to confirm the central role of EGFR pathway activation in the induction of osteoclastogesis, we tested the effects of Erlotinib in the osteoclasts differentiation mediated by NSCLC exosomes. The co-treatment of pre-osteoclasts with exosomes and Erlotinib reverted the effect on exosomes in osteoclasts differentiation, indicating that the block of EGFR pathway inhibited osteoclastogenesis. In order to test if exosomal AREG was an important molecule in the induction of EGFR pathway, we performed experiments with recombinant AREG and AREG neutralizing antibody. The treatment of pre-osteoclasts with recombinant AREG had the similar effects of NSCLC-exosomes on the induction of EGFR phosphorylation causing an increase of RANKL that modulated MMP9 and TRAP expression and induced the typical phenotype of mature osteoclasts. The co-treatment of pre-osteoclasts with NSCLC-exosomes and AREG neutralizing antibodies reverted the effects on osteoclasts differentiation mediated by NSCLC exosomes. The central role of exosomal AREG in osteoclast differentiation was confirmed by a knockdown of AREG in CRL-2868 cells. The decrease of AREG levels in CRL-2868 cells inhibited the accumulation of this molecule into exosomes, reverting the effects on osteoclastogenesis induced by lung cancer exosomes. We demonstrated that NSCLC patient exosomes were enriched in AREG and the data obtained in Raw 264.7 cells treated with exosomes released by CRL-2868 cell line were also confirmed with human committed preosteoclast PMBCs treated with esosomes isolated from plasma of twenty NSCLC patients at different disease stages. **Conclusion:** Our results show that exosomal AREG induces the activation of EGFR pathway that increases, in pre-osteoclasts treated with NSCLC-exosomes, the expression of RANKL at mRNA and protein levels. RANKL, in turn is able to induce the expression of proteolytic enzymes considered osteoclastogenesis markers, triggering the vicious cycle. These data suggest that investigate the role of AREG contained in NSCLC-exosomes in the osteoclast differentiation might permit to improve the therapeutic strategy to inhibit the fatal attraction between lung cancer and bone.

CHAPTER 1

Background

1.1 Lung cancer

Lung cancer represents the main cause of world cancer-related deaths (1). Malignant lung tumors can be subdivided into small-cell-lung carcinoma (SCLC) and non-SCLC (NSCLC). The three main subtypes of NSCLC are: squamous cell carcinoma, adenocarcinoma and large lung cell carcinoma. Almost 85% of lung cancers are classified as NSCLC and adenocarcinoma is the most frequent subtype (2). The lack of clinical manifestations during the initial stages of lung cancer development, the absence of appropriate diagnostic, prognostic and predictive biomarkers and the limited efficacy of the available treatments correlate to high mortality rate (3). Lung cancer preferentially metastasizes in bone, brain, liver and distant lymph nodes (4). NSCLC-patients show bone metastasis at diagnosis or develop bone metastasis during the course of disease (5). Lung cancer induces both osteoblastic and osteolytic metastases formation being osteolytic metastases the most common in NSCLC (6,7). Conventional chemotherapy, in combination with radiotherapy, are the two major treatments to prolong the survival of NSCLC patients (8). These treatments have improved outcomes, but a significant proportion of NSCLC patients do not respond to these treatments. The discovery of new molecular targets (EGFR mutations and ALK rearrangements) and drugs like tyrosine-kinase inhibitors (TKIs) has ameliorated clinical outcomes of the disease. Despite the remarkable initial response, essentially all these tumors recur and eventually develop secondary resistance mutations in the same target, or different alterations in other molecular pathways leading to unsuccessful treatment and disease progression (8). The elucidation of resistance mechanisms to molecular treatment may provide a basis for the development of new strategies to overcome this resistance and to enhance NSCLC patients outcome.

1.2 Epidermal growth factor receptor

Epidermal growth factor family of receptor tyrosine kinases (ErBs) play an essential role in cancer biology. ErBs family consists of four members: EGFR (ErbB1, HER1), ErbB2 (HER2), ErbB3 (HER3) and ErbB4 (HER4). Epidermal growth factor receptor (EGFR) signaling regulates different steps of tumor progression by stimulating uncontrolled proliferation of tumor cells, conferring the ability to evade programmed cell death, promoting their migration in order to facilitate metastasis and angiogenesis, inducing resistance to cytotoxic chemotherapy (9). EGFR is a 486 amino-acid single chain transmembrane glycoprotein of 170 kDa, consisting of an extracellular ligand-binding ectodomain, a transmembrane domain, a short juxtamembrane section, a tyrosine kinase domain and a tyrosine-containing C-terminal tail. The kinase activity, required for signal transduction, is dependent on a lysine residue at position 721 (10). EGFR is regulated by a family of seven peptide growth factors: amphiregulin (AREG), betacellulin (BTC), epidermal growth factor (EGF), epigen (EPGN), epiregulin (EREG), heparin-binding EGF-like growth factor (HBEGF) and transforming growth factor-alfa (TGFA) (10). The soluble form of these growth factors contains a conserved structure known as the EGF-like domain and derived from a transmembrane precursors following a proteolytic cleavage (10). Unstimulated EGFR is a monomer, but forms either homo-or-heterodimers with other EGFR family members, binding soluble ligands to its ectodomain. Receptor dimerization is essential for intracellular tyrosine kinase domains activation, that in turn induces autophosphorylation of C-terminal tyrosines (11,12). The C-terminal phosphotyrosine residues can bind to particular cytoplasmic proteins to amplify mitogenic signalling. Docking proteins such as GRB2 contain an SH2 domain that binds to the phosphotyrosine residues of the activated receptor. GRB2 SH3 domain binds to the guanine nucleotide exchange factor SOS. When the GRB2-SOS complex docks to phosphorylated EGFR, SOS becomes activated. Activated SOS promotes RAS activation, that activates the protein kinase activity of RAF kinase, followed by MEK phosphorylation and mitogen-activated protein kinase (MAPK) activation (13,14,15). This signaling pathway, involved in cellular proliferation regulation, has been proposed as the major mitogenic signalling pathway initiated by the EGFR family of kinases (16). Furthermore, PI3K pathway, is activated, inducing an increase of its downstream effector protein kinase-B (AKT), driving the expression of anti-apoptotic molecules, such as the inhibitor of apoptosis protein survivin (17,18). Another important downstream target is the mTOR pathway, often constitutively active in cancer, implicated in cell cycle progression, apoptosis, and metastasis. Finally, STAT signaling is also regulated by EGFR signaling (19).

1.3 Epidermal growth factor receptor mutations in lung cancer

In lung cancer, specifically in adenocarcinoma, the epidermal growth factor receptor (EGFR) signaling is upregulated, making it an attractive molecular target for tumor treatment (20). The era of molecular targeted therapy in lung cancer started in 2004, when a correlation between clinical response to EGFR tyrosine kinase inhibitors (TKIs) and EGFR activating mutations was observed (21,22). Tyrosine kinase inhibitors (TKIs) are small ATP-competitive molecules that bind to the intracellular tyrosine kinase domain of EGFR, blocking autophosphorylation of EGFR with subsequent inhibition of the downstream signaling cascade. Two first-generation reversible EGFR tyrosine kinase inhibitors (TKIs) were initially approved for lung cancer treatment: Gefitinib and Erlotinib (23,24). Gefitinib (Iressa, ZD1839) was the first oral drug approved by the U.S. Food and Drug Administration (FDA) in May 2003. Erlotinib (Tarceva) was approved by FDA in November 2004. Clinical responses to EGFR TKIs are correlated with mutation in kinase domain-encoding region of the EGFR gene (25). Activating mutations identified in tyrosine kinase domain of EGFR, determine the constitutive activation of the kinase, modifying the autoinhibited conformation (26,27,28), normally maintained in the absence of ligand stimulation. Most clinically-relevant predictor of EGFR-TKIs sensitivity consists of a single point mutation that substitutes Leucin-858 with arginine (L858R) in exon 21 and in-frame deletions in the conserved LREA motif of exon 19 (residues 747-750) (29). In particular, EGFR exon 19 deletion (del746-750) confers more susceptibility to gefitinib treatment compared with tumors with the point mutation (L858R) in exon 21 (30,31). The oncogenic property of the L858R mutation has been demonstrated by the crystal structure and kinetic characterization of the mutant L858R EGFR kinase domain, showing that it has greater activity than WT EGFR (32,33,34). The altered conformation of the mutant tyrosine kinase pocket confers sensitivity for two reasons, I) decrease the affinity of the kinase for ATP (35,36,37,38) with which the inhibitors compete for binding; II) the active state of the kinase facilitates the recognition by TKIs (37,38,39). Most EGFR mutant lung adenocarcinomas that initially show a TKIs remarkable response, often recur, due to acquired EGFR resistance mutations. The most known acquired mutation is located in EGFR gene, exon 20, and replaces methionine for a threonine (T790M) (40), resulting in increased ATP affinity of the kinase. A group of new generation EGFR-TKIs irreversibly bind the EGFR tyrosine kinase, thus representing an attempt to overcome the acquired resistance to first-line generation TKIs and obtaining better outcomes than reversible inhibitors (gefitinib and erlotinib) in lung cancers treatment. The second-generation EGFR-TKIS are: afatinib (GIOTRIF) and dacomitinib (PF-00299804). Afatinib has been approved for treatment of advanced NSCLC, harboring activating EGFR mutations, specifically exon 19

deletions or exon 21 (L858R) mutations. Third-generation irreversible EGFR-TKIs Osimertinib (AZD9291), CO-1686, and HM61713 inhibit both EGFR activating and resistance mutations, showing in early-phase studies promising response against tumors with acquired EGFR T790M. (41).

1.4 Non-EGFR molecular alterations in lung cancer

EGFR gene mutations, and the consequent activation of survival pathways can contribute to EGFR TKIs resistance. In particular, MET receptor gene amplification and protein overexpression have been reported in lung adenocarcinomas and are correlated with a reduction in effectiveness of EGFR inhibitors (42). The hepatocyte growth factor (HGF) and its receptor, the transmembrane tyrosine kinase cMET, promotes cell proliferation, survival, motility, and invasion. Data in literature showed that amplification of MET gene was identified in 22% of patients of a small group of 18 lung adenocarcinomas, which after initial EGFR TKIs treatment developed resistance (43). Recent experimental data also suggested that concomitant inhibition of MET and EGFR signaling in MET-amplified and EGFR-mutated xenografts resulted in an eradication of these tumors (44). Yu et al., showed that another mechanism of acquired resistance is HER amplification. However, there aren't reliable data able to exclude that HER2 amplification was present before acquired EGFR TKI resistance (45). Recent data suggests also that PTEN is implicated in EGFR TKI-resistant lung cancer. Loss of PTEN activity causes an EGFR-independent activation of the PIK-3 signaling axis. EGFR phosphorylation may be increased in the absence of PTEN activity. Further studies are necessary to define the role of PTEN in EGFR TKI resistance pathobiology (2). Other mechanisms of developing resistance to TKIs include constitutive activation of downstream mediators. In lung cancer, particularly in NSCLC, *KRAS*, a main downstream signaling molecule in the EGFR pathway, is frequently affected by somatic point mutations in codon 12 and 13, located in exon 2. KRAS gene encodes for the GTP-binding protein RAS; mutated RAS loses its GTPase activity, becoming constitutively active, leading to activation of downstream pathways including the RAF-MEK-ERK (MAPK) signaling pathway and AKT-PI3K-mTOR pathway. Pao et al. reported for the first time that lung adenocarcinoma patients with *KRAS* mutations are not responsive to gefitinib or erlotinib (46). KRAS mutation correlates to EGFR-TKI therapy nonresponse for EGFR signaling independent pathway activation (2,47). Mutations in BRAF, an ERK (extracellular signal-regulated kinases) signaling pathway component, occur in lung adenocarcinomas, with V600E as the most common mutation. BRAF mutations are usually mutually exclusive with EGFR and KRAS mutations but the role of these mutations in the EGFR TKI therapy remains to be elucidated (2). Moreover, ALK fusion is identified as the second most frequent independent oncogenic driver in

NSCLC (48). Contrarily, Sweis et al. identified concurrent EGFR mutation and ALK translocation in four cases of NSCLC for a total of 20 cases (49). The fusion between echinoderm microtubule-associated protein-like 4 (EML4) gene and anaplastic lymphoma kinase (ALK) gene has recently been identified in a subset of non-small cell lung cancers (NSCLC). The fusion protein EML4-ALK, identified by Soda et al (50) induces a constitutive activation of the intracellular domain of the kinase ALK, that leads to a downstream cascade of events causing carcinogenesis (51). The patients with ALK translocation respond to ALK tyrosine kinase inhibitors, such as Crizotinib® (52).

1.5 Lung cancer bone metastases

The skeleton represents a preferential site for lung cancer metastases, (53,54) but the molecular mechanisms that regulate this process remain poorly understood, and successful treatment are lacking. Lung cancer induces the formation of both osteoblastic and osteolytic metastases and, in NSCLC, lytic bone metastasis are the most common (6,7). Normal bone structure remodelling is dependent on a perfect balance between osteoclast-regulated bone resorption and osteoblast-regulated bone formation (55). Bone-forming cells (osteoblasts) derive from pluripotent mesenchymal stem cell (MSC) (56); while bone-resorbing cells (osteoclasts) originates from proliferation and fusion of monocyte/macrophage precursor cells to form multinucleated cells (56). The key mediator of bone remodelling is RANKL/RANK/OPG system. Receptor-Activator-of-Nuclear-factor-Kappa-B-Ligand (RANKL), a membrane-bound protein expressed on the osteoblasts binds RANK (the receptor activator of nuclear factor NF-Kb) on the surface of osteoclast precursors, stimulating their differentiation into mature osteoclast. Mature osteoclasts, through their podosomes form an acidified compartment known as "resorption pit" on the bone surface. In this space the bone resorbing cells secrete hydrogen ions (H+), which are produced via carbonic anhydrase II (CAII) and delivered into the "resorption pit" through an electrogenic vacuolar-type H+-ATPase (V-ATPase) proton pump. Osteoclasts also secrete high concentrations of proteolytic enzymes such as Cathepsin K (CTSK), tartrate-resistant Acid Phosphatase (TRAP) and Matrix Metalloproteinases 9 (MMP9) (57). The low pH and secretion of enzymes to the bone surface is essential to create optimal conditions for bone organic matrix degradation (58,59). The resorptive function of mature osteoclasts is specifically regulated; an excessive osteoclastogenesis and bone destruction is counteracted by OPG, a decoy receptor of RANKL, also produced by osteoblasts. OPG, blocking RANKL and RANK binding, inhibits osteoclast differentiation and activation (60-62). Soluble factors released from NSCLC cells increase osteoclast activity through the shift of the normal balance between RANKL and Osteoprotegerin (OPG) (63). This bone destructive process induces a “vicious cycle” in which growth factors released by the osteoclasts are able to stimulate

tumor growth and molecules released by cancer cells in turn enhance the osteoclast differentiation. Data in the literature showed the correlation between RANKL/RANK/OPG system expression and lung cancer bone metastases, suggesting it as a therapeutic target. Peng et al., analyzed the RANKL/RANK/OPG system expression in different lung cancer cells (PG-BE1, PG-LH7 and PAa cell lines) with different metastatic potentials. They showed that PG-EB1, the cell line with the highest metastatic potential, exhibited the strongest expression of RANKL, RANK and OPG and a significantly higher RANKL/OPG ratio at both mRNA and protein levels compared to other cell lines. Furthermore, it was demonstrated that human tissue sections from bone metastases originating from NSCLC exhibited higher RANKL: OPG ratio compared with tissue sections from primary NSCLC lesions (63). Karapanagiotou EM et al., showed increased serum levels of osteoclast regulatory protein sRANKL in NSCLC patients with bone metastasis. A clinical correlation between RANKL/OPG/RANK expression with tumor stage, lymph-node metastasis, and distant metastasis was also showed by the authors (64). Data reported in the literature also showed the involvement of RANKL-RANK system in lung cancer cells metastatic potential promotion, suggesting that the migration of NSCLC from primary sites to metastatic nodes might depend on RANKL level. Peng et al., showed that recombinant RANKL protein treatment and transfection with RANKL cDNA stimulated the migration and invasion *in vitro* of least invasive lung cancer PAa cells line expressing RANK. The effect of RANKL *in vitro* was counteracted by OPG addition to the culture medium in a dose-dependent manner (63). The authors obtained similar results *in vivo*, establishing a xenograft mice model by intratibial injection of PAa cells or PAa-RANKL cells. The volume of tumor derived from PAa-RANKL cells was significantly larger than that are derived from PAa cells alone; OPG subcutaneously injected reverted these effects (63).

1.6 The EGFR network in bone biology and pathology

Several reports indicated that EGFR signaling is upregulated in NSCLC and in a variety of tumors metastasizing to the bone (20,65-67). EGFR signaling components are expressed in skeletal cells (68) and play an essential role in bone metabolism by regulating both osteoblasts and osteoclasts activity through a cross talk with RANK/RANKL system. Zhu et al., showed that EGF-like ligands stimulate osteoclast formation by inhibiting the expression of osteoprotegerin (OPG) and by increasing the expression of RANKL and monocyte chemoattractant protein 1 (MCP1) in osteoblastic cells (69). MCP-1 attracts osteoclast precursors to osteoblasts and induce osteoclast fusion and activation (70). EGF and AREG stimulate preosteoblastic cells proliferation but inhibit their differentiation into osteoblastic cells, inducing decreased mature osteoblast number and promoting osteolytic lesions (71-78). The role of EGFR in regulating osteoclasts activity is also

reported in the literature. Recently, it was demonstrated that EGFR is expressed in pre-osteoclasts and EGFR signaling is necessary for osteoclast formation from bone marrow precursor cells (79,80). Data in the literature reported the role of EGFR ligands such as EGF and TGFA in enhancing bone resorption *in vitro* and *in vivo* through osteoclast proliferation induction (81-87).

1.7 Exosomes: structure and biogenesis

Extracellular vesicles (EVs) are classified by different nomenclatures based on their size, intracellular origin and releasing mechanism. The two classes of EVs better characterized are exosomes and microvesicles (88). Microvesicles shed directly from plasma membranes and are characterized by a diameter of 100 nm-1 mm; exosomes are distinct from other EVs for their origin, size, function and composition (89). The term exosome was first proposed in 1983 in Rose Johnstone's laboratory (90), to describe small vesicles (diameter of 20-100 nm) of endosomal origin that were released during reticulocyte maturation (88). To date, the mechanism of exosomes biogenesis is still unclear and known ways of exosomal generation are suggested by literature data. These nanovesicles originate from multivesicular bodies (MVBs), formed during the maturation of early endosomes into late endosomes with the accumulation of intraluminal vesicles (ILVs) and are released into the extracellular space after fusion of MVBs with plasma membrane (90). The Endosomal Sorting Complexes Required for Transport (ESCRT)-dependent mechanism plays a central role in MVB formation, sorting and secretion (91-93) and consists of four distinct complexes (ESCRT-0, ESCRT-1, ESCRT-II, ESCRT-III) with other auxiliary proteins among which Vps4. The ESCRT-0 controls the cargo clustering in a ubiquitin dependent manner, the ESCRT-I and II induce the bud formation in the MVB and the ESCRT-III induces the vescicle scission from the MVB membrane. The auxiliary VPS4 protein plays a role in recycling the ESCRT machinery (94). Once the exosomes are in the luminal space of the MVBs, SNARE family, and concretely, VAMP-7 could enhance the membrane fusion between the MVBs and the plasma membrane (95,96). The ESCRT-independent mechanism requires the sphingolipid ceramide, necessary for the budding of intracellular vesicles into the MVB (97). However, due to their common multivesicular body origin, exosomes have a common set of proteins that allow their identification, based on specific surface markers, such as endosomal markers, including tetraspanins (CD9, CD63, CD81), heat shock 70kDa protein 4 (Hsp70), ALG-2-interacting protein X (Alix), tumor susceptibility gene 101 (Tsg101), and MHC classes I and II (98).

1.8 Exosomes and tumor metastasis

Exosomes are cup-shaped nanovesicles with a lipid bilayer, containing a plethora of proteins, including transmembrane receptors, membrane transporters, adhesion molecules, cytoskeletal and heat shock proteins, cytokines, growth factors, lipids, mRNAs, and miRNAs able to influence the phenotype and biological functions of recipient cells (94).

When discovered, in 1983, exosomes were considered as a mechanism through which viable cells discard their "waste products" into extracellular space instead following studies demonstrated the implications of the exosomes in different aspects of tumorigenesis such as immunomodulation (99), pre-metastatic niche formation (100), tumor growth (101), drug resistance (102) and more recently, drug removal (extrusion) (103). Tumor metastasis is a critical step in malignant progression, responsible of failure of cancer therapy and death of a large majority of cancer patients (104). The metastatic process is characterized by interaction of cancer cells with stroma in distant organs and their full colonization, leading to development of the aggressive tumor phenotype (105,106). Metastases are directed to preferential organs; for example prostate cancer to the bones, pancreatic cancer and uveal melanoma to the liver, whereas tumors such as melanoma, breast- and lung cancer can colonize several organs (107).

The Stephen Paget's "seed-and soil" hypothesis suggests a preferential colonization of pre-metastatic niches in distant organs (soil) by circulating tumor cells (CTCs) derived from different tumor types (seed) based on "functional" interactions between tumor cells and target microenvironment (105,106,108-110). Despite Paget's 126 years-old "seed-and-soil" hypothesis (111), metastatic organotropism remained one of cancer's greatest mysteries and insufficient progress has been made to decode the mechanisms governing organ specific metastasis. Several studies support a role for exosomes released by cancer cells as intercellular oncogenic driver of functional biomolecules, in remodeling the tumor microenvironment, providing a hospitable environment ("priming the metastatic niche"), and thereby contributing to tumor progression via enhanced angiogenesis and metastasis. It was demonstrated that exosomes mediated transfer of oncogenic EGFR from human squamous cell carcinoma to tumor-associated endothelial cells activated MAPK and AKT cell signaling pathways and promoted endothelial VEGF expression (112). Melanoma-derived exosomes have recently been shown to promote metastasis through the preparation of the metastatic niche via crosstalk between the released exosomes and bone marrow progenitor cells (113). Raimondi L et al., demonstrated that exosomes released by multiple myeloma cells are involved in osteoclasts differentiation. These exosomes induced the differentiation of murine RAW 264.7 macrophages and human primary preosteoclasts in osteoclasts, increasing the

expression of osteoclast markers such as Cathepsin K (CTSK), Matrix Metalloproteinases 9 (MMP9) and Tartrate-resistant Acid Phosphatase (TRAP) (114). Jung et al, demonstrated in a rat model of pancreatic adenocarcinoma that exosomes of the metastatic adenocarcinoma create premetastatic niches in lymph-nodes and lungs (115) in a CD44v4 dependent manner. Draining lymph-nodes and lung tissue modulation by exosomes released by highly metastatic cells support dissemination of poorly metastatic cells. CD44 is a marker of cancer initiating cells (CICs) that induces metastasis formation by organizing a niche in (pre)metastatic organ (116,117). Furthermore, CD44 protects cells from apoptosis by affecting receptor-mediated apoptosis and by activating antiapoptotic proteins (118,119). EGFR signaling via exosomes might also contribute to metastatic niche formation and cancer promotion (120,121). For the first time, Higginbotham et al., demonstrated that EGFR ligands are released in extracellular vesicles, showing a key role as important actors in metastatic niche preparation (120). The authors showed that two EGFR ligands, HB-EGF and TGFα are released in extracellular vesicles purified from both breast cancer cells MDA-MB-231 cells and HCA-7 colorectal cancer cells whereas AREG was detected only in HCA-7 vesicles. They also demonstrated that treatment with exosomes released from AREG-expressing MDCK (Madin-Darby canine kidney cells) cells induces the highest invasive activity in MDA-MB-231-derived LM2-4175 and LMO-1833 recipient cells that metastasize to lung and bone, respectively (120) compared to exosomes released from TGFα or HB-EGF-expressing MDCK cells. Corrado et al., showed that leukaemic cells (LAMA84) and blood samples of CML patient's exosomes contain amphiregulin (AREG), and are able to activating EGFR signalling in bone marrow stromal cells (HS5), increasing the expression of SNAIL and its targets, MMP9 and IL8. IL8 secretion from stromal cells promote proliferation and survival of leukaemic cells, both *in vitro* and *in vivo* establishing a bidirectional crosstalk. Pre-treatment of HS5 with LAMA84 exosomes increases the expression of annexin A2, promoting leukaemic cells adesion to stromal monolayer, supporting the growth and invasiveness of leukaemic cells (121).

In particular, Amphiregulin (AREG) is overexpressed in several cancers such as colon, breast and lung (122). Moreover, its levels in plasma of NSCLC patients correlate with poor prognosis (123).

1.9 Exosomes-based biomarker analysis in lung cancer disease

Although different therapeutic strategies, including surgery, radiation, chemotherapy, and targeted molecular therapy are commonly used in lung cancer treatment, either alone or in combination, the prognosis for lung cancer is still poor, due primarily to therapeutic resistance and high metastasis rates (124). Unfortunately, have a tissue sample to monitor lung cancer disease progression is still a main problem, especially during recurrence; for this reason new non-invasive early diagnostic, predictive and prognostic biomarkers are needed (125,126). Recently, the implementation of liquid biopsies in diagnosis, prognosis and follow-up of lung cancer patients has proven to be feasible and of great clinical interest (127,128). In particular, exosomes can be used as biomarkers for early detection, monitoring and prognosis of lung cancer disease (129-131). The goals of exosomes-based biomarker analysis is the significant reduction of sample complexity, when compared to whole body fluids and the reduction of invasiveness in a "liquid biopsy scenario" (132). Exosomes are highly stable in biological fluids and are protected from degradation by their lipid bilayer (133). They have been implicated in several cellular functions and their cargo may be deregulated in disease, regarding it as ‘snapshots’ of their producer cells (134). These vesicles have been described in numerous biological fluids, such as blood (serum and/or plasma), breast milk, urine, amniotic fluid, saliva, cerebrospinal fluid, nasal secretions, bronchoalveolar lavage, bile, synovial fluid, sperm, malignant effusions and ascites (98-135,136).

1.10 Exosomes in lung microenvironment and pathogenesis: Exosomes as biomarkers in lung cancer

Exosomes purified by lung cancer cells and biological fluids of patients with NSCLC can offer a great deal of biological information about physiological and pathological condition's patients, becoming indicative for the early detection, monitoring and prognosis of lung cancer disease as described in the literature data. The utility of miRNAs for cancer study has been largely described (137). Despite circulating miRNAs are promising next-generation biomarkers for lung cancer disease, few studies related to circulating extracellular vesicles miRNAs in lung cancer have been reported. MicroRNAs (miRNAs) are small non-coding RNAs. They are recognized to regulate a number of genes by binding to the 3’UTR of their target mRNA, resulting in the alteration of the targeted gene expression. A single miRNA can influence multiple genes in a single cell. Rabinowits et al., in 2009, demonstrated the potential application of exosomal miRNAs as biomarker for lung cancer. The authors compared 12 miRNAs (miR-17-3p, miR-21, miR-106a, miR-146, miR-155, miR-191, miR-203, miR-203, miR-205, miR-210, miR-212, and miR-214) in peripheral circulation

exosome-derived miRNAs and tumor-derived miRNAs in lung cancer patients and healthy donors. The results showed no significant difference between peripheral circulation miRNA-derived exosomes and miRNA-derived tumors. These miRNAs (miR-17-3p, miR-21, miR- 106a, miR-146, miR-155, miR-199, miR-192, miR-203, miR-205, -miR 210, -miR -212 and miR -214) were present in NSCLC both in tissue and in circulating exosomes but their levels were non-detectable in healthy donors, suggesting their application as predictive biomarkers of NSCLC (138). Cazzoli et al., screened 746 miRNAs in circulating exosomes analyzed on a training set of 3 groups: Lung Adenocarcinomas, Lung Granulomas, healthy former smokers. The authors selected 4 exosomal miRNAs (miRNA-378a, miR-379, miR-139-5p, and miR-200b-5p) as screening markers for segregating lung adenocarcinoma and carcinomas patients from healthy former smokers. They also identified six potential diagnostic exosomal miRNAs (hsa-miR-151a-5p, -30a-3p, -200b-5p, -6299, -100, and -154-3p) that discriminate between lung adenocarcinoma and granuloma. These profiles were confirmed in a validation set of 50 patients (139). As mentioned earlier, one of the main problem of NSCLC is the high rates of progression and recurrence of the patients and exosomes are regarding as new non-invasive biomarkers useful to monitor disease progression. Several miRNAs have been reported to be indicative of tumour progression before Computerize Tomography Scan (CT) detection. The downregulation of the miRNA-146-5p is indicative of a poor progression free survival (PFS) compared to those patients with higher levels of the miRNA inside the exosomes (140). Exosomal miRNAs have been described also as predictive biomarkers for treatment response, considering them useful to improve clinic treatment choice. miRNA-145-5p levels are correlated to the tumour chemosensitivity to cisplatin mediated through the blockade expression of Atg12, an autophagy mediator gene (140). Two other independent studies show that upregulation of miR-1246 and miR-208-a is correlated with a high proliferation of the tumour and a resistant profile to radiotherapy by targeting the genes DR5 and p21 respectively (141,142). The discovery of NGS (Next-Generation Sequencing) has allowed to consider also exosomal RNAs and DNAs as a real alternative to the tissue analysis. Rolfo C et al., described for the first time the ALK-EML4 chromosomal translocation inside the exosomes in 17 advanced NSCLC patients, showing a positive correlation with tissue from the same patients for 14 sample analyzed (143). Recent studies have performed a proteomic profile of tumor-derived exosomes showing exosomal enrichment of several proteins. Lung cancer exosomes contain several tumour associated proteins as reported in literature data. Park et al performed the proteomic analysis of EVs derived from pleural effusion of NSCLC patients, showing that microvesicles contained 912 different proteins, including the epidermal growth factor receptor (EGFR), K-Ras, basigin (EMMPRIN, CD147), carcinoembryonic antigen-related cell adhesion molecule 6 (CEACAM6), claudin1, claudin 3, and RAB family proteins (144).

It has been reported that some EV proteins, such as leucin-rich alfa2-glycoprotein (LRG1), EGFR, CD91, and CD317, may be potential exosomal markers of NSCLC (145-148). In particular exosomal EGFR has been evaluated in NSCLC. Yamashita et al., detected the presence of exosomal EGFR in five out of nine plasma samples from NSCLC patients, but none in nine healthy controls (146). Similarly, in tumour biopsies, Huang et al. found exosomal EGFR in 80% of patients with NSCLC, but only in 2% of patients with chronic obstructive lung disease (147). Sandfeld-Paulsen et al. in a study with 276 NSCLC patients of all stages identified 49 exosomal membrane-bound proteins and among these, 9 proteins with potential prognostic potential in NSCLC. In particular, they indicate NY-ESO, EGFR and PLAP as prognostic markers for decreased survival with increasing concentration level in NSCLC (149). Nowadays, the methodology that focus only on a single exosome-protein has been overtaken by multiple protein markers panel (150). A recent study used an extracellular vesicle array with 49 antibodies. Among the 49 exosomal proteins, CD151, CD171, and tetraspanin 8, have been considered the strongest markers to identify lung cancer of all histological subtypes compared to control samples (151).

1.11 Rational and Objectives

The main objective of my research project is to understand the role played by non-small cell lung cancer (NSCLC)-derived exosomes in bone metastasis formation. We hypothesize a role of NSCLC-exosomes, containing AREG, in EGFR pathway activation in pre-osteoclasts, that in turn causes an increased expression of RANKL. RANKL is able to induce the expression of proteolytic enzymes, well-known markers of osteoclastogenesis, triggering a vicious cycle in lung cancer osteolytic bone metastasis. The experimental model consists of two cell lines: CRL-2868, a NSCLC cell line, istotype adenocarcinoma, sensitive to the first generation TKIs (Erlotinib and Gefitinib) and RAW 264.7, a macrophage murine cell line, precursor of osteoclasts. The experimental strategy was to isolate CRL-2868-derived exosomes and to treat RAW 264.7 cells with exosomes in order to evaluate the role of exosomal-AREG in osteoclastogenesis induction through EGFR pathway activation. The aims of this thesis can be subdivided into five subsequent steps:

1.To investigate the role of CRL 2868-exosomes in osteoclast differentiation through gene and protein modulation of osteoclastic differentiation markers (TRAP, CATHEPSIN and MMP9) in RAW 264.7 cell line.
2. To investigate the role of AREG carried by CRL2868-exosomes in EGFR pathway activation and subsequent osteoclasts differentiation.
3. To investigate the role of AREG knockdown, neutralizing antibodies for AREG and the co-treatment with NSCLC-exosomes and Erlotinib in abrogating the effects induced by CRL 2868-exosomes in osteoclast differentiation.
4. To investigate the role of AREG contained in exosomes released in lung cancer patients's plasma at different stages of tumor's progression in human osteoclast differentiation.
5. To investigate the role of AREG as a predictor of bone metastases induced by lung cancer through the isolation of exosomes released by different cell lines: cell lines that do not metastasize the bone (SW620, K562), cell lines that metastasize the bone (MDA-MB-231, PC3, A549), non-tumor cell lines (HS5, HEK-293).

CHAPTER 2

Materials and Methods

Cell culture and reagents

Non-small cell lung cancer, CRL-2868 cell line was obtained from Prof Christian D. Rolfo (University Hospital Antwerp Oncology). CRL-2868 cells were grown in RPMI-1640 (Euroclone, UK) supplemented with 10% Fetal Bovine Serum (FBS, Euroclone, UK), 100 U/ml penicillin and 100 µg/ml streptomycin (Euroclone, UK) and with 1% Sodium pyruvate (Euroclone, UK). Non-small cell lung cancer, A549 cell line and prostate cancer, PC3 cell line were obtained from ATCC and were grown in RPMI-1640 (Euroclone, UK) supplemented with 10% Fetal Bovine Serum (FBS, Euroclone, UK), 100 U/ml penicillin and 100 µg/ml streptomycin (Euroclone, UK). Breast cancer, MDA-MB-231 cell line was obtained from ATCC and grown in DMEM-F12 (Euroclone, UK) supplemented with 10% Fetal Bovine Serum (FBS, Euroclone, UK), 100 U/ml penicillin and 100 µg/ml streptomycin (Euroclone, UK). Murine macrophage Raw 264.7 cells were purchased from ATCC® and cultured in Dulbecco's modified Eagle's medium (DMEM), supplemented with 10% FBS, 100 U/ml penicillin and 100 µg/ml streptomycin. To induce differentiation, RAW 264.7 cells were treated with 25 ng/ml of human recombinant RANK Ligand (RANKL) (Gibco, Life Techonologies, USA) for 6 days in DMEM, supplemented with 10% FBS, previously ultracentrifugated (OC medium). Alternately, cells were treated for 6 days with 20 µg/ml and 50 µg/ml of CRL-2868 cell-derived exosomes (CRL-2868-exosomes), in DMEM, supplemented with 10% of ultracentifugated FBS. Erlotinib (Cayman Chemical, Ann Arbor, MI, USA) was solubilized at 10 mM stock solution in DMSO and stored at −20 °C. Neutralizing antibody anti-AREG (R&D Systems, Abingdon, UK) was reconstituted at 0.2 mg/ ml in sterile PBS, aliquoted and stored at −20 °C. Recombinant AREG (R&D Systems, Abingdon, UK) was reconstituted at 0.1 mg/ml in sterile PBS, aliquoted and stored at −20 °C. Working dilutions, where necessary, were prepared in medium.

Isolation of human peripheral blood mononuclear cells

Human blood samples were obtained from two healthy donors, after written informed consent obtained in accordance with the Declaration of Helsinki guidelines and Antwerp University Ethics committee n. 14/17/206. Human peripheral blood mononuclear cells (PBMCs) were isolated using the Ficoll-Paque (GE Healthcare Bio Science, Uppsala, Sweden) separation technique.

Preparation of human primary preosteoclasts (pOCs) and osteoclasts (OCs)

PBMCs were cultured in 12-well plates at 1.5×10^6 cells per well in RPMI-1640 supplemented with 10% FBS previously ultracentrifuged, 25 ng/ml of human recombinant RANK Ligand, 25 ng/ml of human MCSF (Gibco, Life Technologies, USA), and 10 nM dexamethasone (Sigma-Aldrich Italy) (Human OC medium). After 2–4 days, the cultures were washed with RPMI-1640 medium to remove non-adherent cells. The adherent cells were mononucleated expressing TRAP and were considered committed pre-osteoclast. For human osteoclastogenesis assays, OC medium was added and the cultures were continued for additional 4 days, at the end of the incubation, they contained large mature multinucleated OCs. The culture period was 6–8 days for both TRAP staining assay and qRT-PCR analysis.

NSCLC patients

Exosomes isolated from human blood samples were obtained from twenty diagnosed NSCLC patients at different disease stages. Informed consent was obtained from patients, according to the Declaration of Helsinki and with hospital ethics committee approval (Antwerp University Ethics committee n. 14/17/206). Plasma patients derived exosomes were isolated as described in the following section "Exosomes isolation". The patient population was selected according to these inclusion criteria: histologically or cytologically confirmed diagnosis of stage III or IV; EGFR mutation status; presence or not of bone metastasis; age 18 years or older at the time of informed consent; smokers and no-smokers declaration, sensitive to first line TKI inhibitors.

Exosomes isolation

Exosomes released from CRL-2868 cells after a 24 hours culture period in the presence of FBS previously ultracentrifugated (vesicle-free media) were isolated from conditioned culture medium (CM) by different centrifugation steps as described by Thery et al. (152): 5 minutes at 300g in order to eliminate cells and debris; 15 minutes at 3000g in order to eliminate apoptotic bodies and 30 minutes at 10.000g in order to eliminate microvesicles. The CM were ultracentrifuged for 100,000 × g for 1 hour and 45 minutes at 4 °C. Exosomes pellet was washed and then resuspended in PBS. In average, we obtained 20 µg of exosomes from 7, 5×10^5 cells and 50 µg of exosomes from 1, 8×10^6 cells. The same exosomes isolation procedure was used for the other cell lines. Exosome protein content was determined by the Bradford assay (Pierce, Rockford, IL, USA). Exosomes from plasma of NSCLC patients (1,5 ml) were isolated after the 100,000 × g ultracentrifugation for 1 hour and 45 minutes at 4 °C to pellet the exosomes. Exosomes pellet was washed and then resuspended in PBS. Exosomes protein content was determined by the Bradford assay (Pierce, Rockford, IL, USA).

Dynamic light scattering (DLS) analysis

Exosome size distribution was determined by DLS experiments. Exosome samples were diluted 30 times to avoid inter-particle interaction and placed at 20°C in a thermostated cell compartment of a Brookhaven Instruments BI200-SM goniometer with a solid-state laser tuned at 532 nm. Scattered intensity autocorrelation functions g2(t) were measured by using a Brookhaven BI-9000 correlator and analyzed in order to determine the distribution P(D) of the diffusion coefficient D by using a constrained regularization method or alternatively a gamma distribution. The size distribution, namely the distribution of hydrodynamic diameter Dh, was derived by using the Stokes-Einstein relation: $D = (kBT)/ (3\pi\eta Dh)$, where D is the diffusion coefficient, kB is the Boltzman constant, η is the medium viscosity and T is the temperature. The mean hydrodynamic diameter of exosomes was calculated by fitting a Gaussian function to the measured size distribution.

Uptake of CRL-2868-exosomes by Raw 264.7 cells

CRL-2868 and A549 cell-derived exosomes were labeled with PKH26 (Sigma-Aldrich, Italy), according to the manufacturer's instructions. Briefly, exosomes collected after the 100,000 × g ultracentrifugation, were incubated with PKH26 for 10 min at room temperature. Labeled exosomes were washed in PBS, centrifugated and resuspended in low serum medium and incubated with Raw 264.7 cells, seeded in 24-well plates at a density of 100.000 cells per well, for 1–3 hours at 37 °C. In

a set of experiments, RAW 264.7 cells were pretreated with 50 μM 5-ethyl-N-isopropyl amiloride (EIPA), a known inhibitor of exosomes uptake, for 3 h. After incubation, cells were processed as previously described (153). RAW 264.7 cells were stained with ActinGreenTM 488 Ready ProbesR Reagent (Life Technologies, USA) that binds F-actin with high affinity. Nuclei were stained with Hoechst (Molecular Probes, Life Technologies, USA) and analyzed by confocal microscopy (Nikon Eclipse Ti). Each picture was acquired with laser intensities and amplifier gains adjusted to avoid pixel saturation. Each fluorophore used was excited independently and sequential detection was performed. Each picture consisted of a z-series of images of 1024–1024 pixel resolution. IMAGE-J software (http://imagej.nih.gov/ij/) was used in order to perform a semi-quantitative analysis of fluorescence intensity; we selected the perinuclear area in a section at 5 μm and measured the fluorescence intensity. Values are the mean ± SD of 15 measurements from three independent experiments.

Transmission electron microscopy (TEM)

Murine macrophage RAW 264.7 cells treated with CRL-2868 exosomes for seven days were analyzed by TEM. After a brief rinse in PBS, cells were fixed with 2.5% glutaraldehyde 0.1 M sodium cacodylate, pH 7.3, for 60 min at room temperature. Cells were then rinsed, post-fixed with 1% osmium tetroxide in the same buffer for 1 h at 4 °C, and dehydrated in ascending alcohols. After embedding in Epon resin, ultrathin sections were cut using a Reichert Ultracut E, stained, and examined using a transmission electron microscope (Jeoll JEM-1400 Plus,), at 80 kV. Images were taken with Digital CCD Camera 8 M. Moreover, for electron microscopic studies, a 5 μl aliquot of exosome preparations was placed onto carbon-coated 200-mesh copper grids (Electron Microscopy Sciences, USA) for 20 min at room temperature. After, the samples were fixed for 5 min in 1% glutaraldehyde in PBS and negatively stained with 2% aqueous solution of phosphotungstic acid. The grids were examined using JEOL JEM-1400 Plus electron microscope, at 80 kV.

Immunogold-labelling of AREG in exosomal membranes (immunoelectron microscopy)

Membrane vesicles were resuspended and applied onto 200-mesh grids with formvar- carbon-coating. The samples were blocked with 1% bovine serum albumin in PBS. The grids were incubated with rabbit Ab against AREG, followed by goat anti-rabbit IgG coupled to 12-nm gold (Jackson). Control grids were also included, in which the primary antibody was omitted. The grids were post-fixed in 1% glutaraldehyde in PBS, negatively stained and examined under Jeoll JEM-1400 Plus electron microscope.

Knockdown of Amphiregulin with shRNA Plasmid in CRL-2868 cells

Stable transfection of Amphiregulin shRNA Plasmid sc-39412-SH (Santa Cruz Biotechnology, Inc.) in CRL 2868 cells was carried out according to the suggestions from Santa Cruz Biotechnology, Inc. Cell line cultures were grown in a six well tissue culture plate, in RPMI medium supplemented with 10% FBS (without standard antibiotics) to reach about 50–70% confluence. The optimal shRNA Plasmid DNA: shRNA Plasmid Transfection Reagent ratio, experimentally determined was 3 µg of shRNA Plasmid DNA and 3 µl of shRNA Plasmid Transfection Reagent. Following incubation for 30 minutes at room temperature, the shRNA Plasmid DNA/ShRNA Plasmid Transfection Reagent Complex was added to CRL 2868 cells. Following incubation for 7 hours at 37 °C in a CO_2 incubator, RPMI medium containing 2 times the normal serum and antibiotics concentration (2x normal growth medium) was added. The cells were incubated for an additional 24 h at 37 °C in a CO_2 incubator. For selection of stably transfected cells, puromycin, at the concentration of 4 µg/ml, was added to the medium 48 hours post-transfection. Every 2 days the growth medium was aspirated and replaced with freshly prepared selective media. Controls shRNA Plasmids included: Control shRNA Plasmid-A (sc-108060), Control shRNA Plasmid-B (sc-108065), Control shRNA Plasmid-C (sc-108066) and cofGFP Control Plasmid (sc-108083).

RNA extraction and realtime PCR

RAW 264.7 cells were cultured in 12-well plates at 5.000 cells/ml for well and treated or not with CRL-2868-exosomes and A549 exosomes (20-50 µg/ml) or recombinant AREG (20-50 ng/ml) or RANK Ligand 25 ng/ml ± Erlotinib 0.5 µM for 6 days, as described in the results section. Neutralizing antibodies anti-AREG (Novus) (20 ng/ml) were incubated with CRL-2868 exosomes or A549 exosomes for 1h at 37°C and then used to treat RAW 264.7 cells for 6 days. As negative control, CRL-2868 exosomes were incubated with non-specific antibodies for 1h at 37°C. Human primary

preosteoclast cells were grown in 12-well plates at 1.5×10^6 cells per well and treated or not with CRL-2868-exosomes (20-50 µg/ml) or recombinant AREG (20-50 ng/ml) or RANK Ligand 25 ng/ml ± Erlotinib 0.5 µM for 4 days, as described in the results. Human primary preosteoclast cells were, also treated with exosomes collected from plasma of patients NSCLC (20 µg/ml) for 4 days, as described in the results. RNA was extracted using the commercially available Illustra RNAspin Mini Isolation Kit (GE Healthcare, Little Chalfont, Buckinghamshire, UK), according to manufacturer's instructions. Total RNA from RAW 264.7 or from human primary preosteoclast cells was reverse transcribed to cDNA using the High Capacity cDNA Reverse Transcription kit (Applied Biosystems, Foster City, CA, USA). RT-QPCR was performed in 48-well plates using the Step-One Real-Time PCR System (Applied Biosystems). For quantitative Sybergreen real-time PCR, reaction was carried out in a total volume of 20 µl containing 2 SYBER Green I Master Mix (Applied Biosystems), 2 µl cDNA and 300 nM forward and reverse primers. Primers were obtained from Invitrogen (Foster City, CA, USA) and Primer sequences are reported in Table 1. Real-time PCR was performed in duplicates for each data point. Relative changes in gene expression between control and treated samples were determined using the Ct method. Levels of the target transcript were normalized to a GAPDH endogenous control, constantly expressed in all samples (ΔCt). For ΔΔCt values, additional subtractions were performed between treated samples and control ΔCt values. Final values were expressed as fold of induction.

Western blotting and antibodies

RAW 264.7 cells were cultured in petri dishes (p100) at 30.000 cells for each and treated or not with CRL-2868 exosomes (20-50 µg/ml) or recombinant AREG (20-50 ng/ml) or RANKL 25 ng/ml ± Erlotinib 0.5 µM for 6 days, as described in the results. Neutralizing antibodies anti-AREG (20 ng/ml) were incubated with CRL-2868-exosomes (50 µg/ml) for 1h at 37°C and then used to treat RAW 264.7 cells for 6 days. SDS-PAGE Electrophoresis and Western Blotting were performed as previously described (4). Briefly, cells were lysated for 1 hour and 30 minutes in lysis buffer containing 15mM Tris/HCl pH7.5, 120mM NaCl, 25mM KCl, 1mM EDTA, 0.5% Triton X100, and Protease Inhibitor Cocktail (100X, Sigma-Aldrich, USA). Cell lysates (from 30 µg to 50 µg per lane) were separated using 4-12% Novex Bis-Tris SDS-acrylamide gels (Invitrogen, Life Technologies, USA), transferred on Nitrocellulose membranes (Invitrogen, Life Technologies, USA), and immunoblotted with the primary antibodies. The following antibodies were used: EGFR, p-EGFR (Cell Signaling Technology, Lane Danvers, MA, USA), AREG (R&D Systems, Abingdon, UK), CD63 (sc-15363), were obtained from Santa Cruz Biotechnology (Santa Cruz Biotechnology, Inc., Santa Cruz, CA, USA); Alix (2171S) antibodies were obtained from Cell Signaling (Beverly, MA).

TRAP staining assay

RAW 264.7 cells and human primary osteoclasts were stained for detection of TRAP activity according to the manufacturer's protocol (Acid Phosphatase, Leukocyte (TRAP) Kit; Sigma-Aldrich, USA) and evaluated by optical microscopy. Raw 264.7 cells were seeded in 12-well plates at a density of 2.000 cells per well and treated for 6 days with CRL-2868 exosomes (20–50 μg/ml), A549 exosomes (20–50 μg/ml), recombinant AREG (20–50 ng/ml) or RANK Ligand 25 ng/ml ± Erlotinib 0.5 μM. Neutralizing antibodies anti-AREG (20 ng/ml) were incubated with CRL-2868-exosomes or A549 exosomes (50 μg/ml) for 1 h at 37 °C and used to treat RAW 264.7 cells for 6 days. Human primary osteoclasts were seeded in 12-well plates at a density of 1.5×10^6 cells per well and cultured in OC medium alone or with CRL-2868-exosomes (20–50 μg/ml) ± Erlotinib 0.5 μM or with plasma patients (NSCLC) derived exosomes (20 μg/ml). TRAP positive multinucleated cells were scored as mature osteoclasts. Three independent experiments were performed in triplicate; cells from five different fields were counted for each condition.

ELISA assay

RAW 264.7 conditioned medium (CM) was collected from cells stimulated or not for 6 days with CRL-2868-exosomes (20-50 μg/ml), recombinant AREG (20-50 ng/ml) or RANKL 25 ng/ml ± Erlotinib 0.5 μM. Neutralizing antibodies anti-AREG (20 ng/ml) were incubated with CRL-2868 cell-derived exosomes (50 μg/ml) for 1h at 37°C and used to treat RAW 264.7 cells for 6 days. Human primary osteoclasts conditioned medium (CM) was collected from cells stimulated for 4 days with OC medium alone or with CRL-2868-exosomes (20-50 μg/ml) ± Erlotinib 0.5 μM or with plasma patients (NSCLC) derived exosomes (20 μg/ml). CM aliquots were centrifuged to remove cellular debris and used to quantify MMP9 and RANK Ligand with ELISA kits according to the manufacturer's protocol. MMP9 levels secreted by both Human primary OCs and Raw264.7 cells were quantified respectively by Human MMP-9 ELISA assays (Invitrogen) and mouse ELISA Kit for MMP9 Cloud-clone Corp®. RANK Ligand levels secreted by both Human primary OCs and RAW 264.7 cells were quantified respectively by ELISA Complete kit human sRANKL assay (KOMABIOTECH) and ELISA Complete kit mouse sRANKL assay (KOMABIOTECH).

CHAPTER 3

Results

3.1 Characterization of exosomes released by NSCLC cells

CRL-2868 cells are able to release nanovesicles into the culture medium, that were isolated by ultracentrifugation for 100,000 × g for 1 hour and 45 minutes at 4°C and characterized as exosomes by Western blotting using antibodies specific for ALIX, TSG 101 and CD63 (Fig. 1a). TEM analysis further showed that vesicles released from CRL-2868 cells, have the well-known cup shape already described for exosomes isolated from different cell lines (Fig. 1b).

3.2 CRL-2868 exosomes contain AREG

Our research group had previously demonstrated that exosomes released by multiple myeloma cells are involved in osteoclasts differentiation. These exosomes induced the differentiation of murine RAW 264.7 and human primary preosteoclasts in osteoclasts, increasing the expression of osteoclast markers such as Cathepsin K (CTSK), Matrix Metalloproteinase 9 (MMP9), and Tartrate-resistant Acid Phosphatase (TRAP) (114).

Our hypothesis is that CRL-2868 exosomal AREG activates the EGFR pathway in RAW 264.7 cells, thus remodelling the bone microenvironment, and "priming the bone metastatic niche" for cancer cells, thereby contributing to tumor progression. In order to confirm our hypothesis we demonstrated, as a first step, a CRL-2868-exosomal enrichment of AREG with respect to parental cells, as demonstrated by Western blotting using antibody specific for AREG (Fig. 1c). TEM analyses following immunogold-labelling showed that AREG decorates the CRL-2868 exosomal membranes (Fig. 1d).

3.3 CRL-2868 exosomes are internalized by Raw 264.7 cells and induce morphological differentiation of murine preosteoclasts

The uptake of isolated exosomes by Raw 264.7 cells was examined by labelling exosomes with PKH-26: RAW 264.7 cells treated with CRL-2868 exosomes internalized the vesicles in a time and dose-dependent manner (Fig. 2). As shown in Figure 2, exosomes are rapidly internalized by Raw 264.7 cells at 37°C and localized in the perinuclear compartment after 3 hours of incubation. Figure 3 shows that the addition of CRL-2868 exosomes to RAW 264.7 cells positively modulates cell differentiation in mature osteoclasts, inducing the typical multinucleated osteoclast morphology. Treatment of preosteoclasts was done with 20 μg/ml of CRL-2868 exosomes for 6 days. In Fig. 3a confocal analyses showed the induction of multinucleated cells and filopodia formation. Furthermore, in order to evaluate the differentiation toward a mature osteoclast phenotype we analyzed the ultrastructural morphology of cells at TEM. In the control culture (untreated RAW 264.7 cells), cells displayed the typical features of monocytes with smooth cell surfaces. On the contrary, multinucleated cells of various size and morphology were observed among monocytes grown in the presence of CRL-2868 exosomes (Fig. 3b). The multinucleated osteoclasts were structurally characterized by the development of ruffled borders; they exhibited large nuclei with several nucleoli. In the cytoplasm, we observed a rich rough endoplasmic reticulum, mitochondria and many lysosomal bodies (Fig. 3b). We also observed that exosomes released by A549, another NSCLC cell line, are uptaken by RAW 264.7 cells in a time and dose dependent manner (Fig. 4a) and are able to induce osteoclast differentiation similarly to exosomes released by CRL-2868 cells, inducing multinucleated morphology of pre-osteoclasts, typical of mature osteoclasts (Fig. 4b).

However, the uptake of CRL-2868 and A549 exosomes in RAW 264.7 cells was blocked by treatment of pre-osteoclasts with 50 μM EIPA (Fig.5a), a well-known blocker of macropinocytosis, thus supporting the hypothesis that exosomes internalization could occur by endocytosis. Semi-quantitative analysis of PKH-26-exosomes fluorescence intensity in the cytoplasm of RAW 264.7 cells is showed in Figure 2b and 5b.

3.4 CRL-2868 exosomes induce the activation of EGFR pathway

It was demonstrated that EGFR is expressed in pre-osteoclasts and EGFR signaling is necessary for osteoclast formation from bone marrow precursor cells. EGFR ligands stimulate osteoclast formation by inhibiting OPG expression and upregulating RANKL (69). We demonstrated that the addition of CRL-2868 exosomes to RAW 264.7 cells induced the activation of EGFR pathway and osteoclast markers expression. As shown by Western blotting analysis, RAW 264.7 cells treated for 6 days, with 20 μg/ml CRL-2868 exosomes (Exo) and RANKL (positive control) showed an increase of EGFR phosphorylation (pEGFR) compared to untreated cells (Ctrl) (Fig. 6a and b). The role of EGFR pathway activation in osteoclast differentiation was investigated, focusing our attention on RANKL modulation by CRL-2868 exosomes. RANKL is a membrane-bound protein expressed on osteoblasts that binds RANK, on the surface of osteoclast precursors, stimulating their differentiation into mature osteoclast, increasing the expression of osteoclast markers, such as Cathepsin K (CTSK), Matrix Metalloproteinase 9 (MMP9) and Tartrate-resistant Acid Phosphatase (TRAP). Interestingly, through quantitative Real Time PCR analysis, we demonstrated an increase of msRANKL gene expression in Raw 264.7 cells treated for 6 days, with 20 and 50 μg/ml CRL-2868 exosomes compared to untreated cells (Fig. 6c). These data were confirmed also at protein level with an ELISA assay: treatment of Raw 264.7 with CRL-2868 exosomes for 6 days, with 20 and 50 μg/ml CRL-2868 exosomes increased the amount of soluble msRANKL in culture medium (Fig. 6d). In order to investigate the role of CRL-2868 exosomes in EGFR pathway activation, as first step we demonstrated, by western blotting analysis, that CRL-2868 exosomes didn't show an EGFR exosomal enrichment compared to parental cells (Fig 6e). These data indicate that CRL-2868 exosomal AREG induces EGFR pathway activation and the endogenous upregulation of RANKL in osteoclast precursors, suggesting the role of CRL-2868 exosomes as osteoclastogenesis inducers.

3.5 CRL-2868 exosomes induce osteoclast differentiation markers expression

The differentiating effect mediated by EGFR pathway activation, were also analyzed through analysis of TRAP and MMP9 expression, well-known genes involved in osteoclasts differentiation. Through qPCR analysis, we demonstrated an increase of TRAP and MMP9 gene expression in Raw 264.7 cells treated for 6 days, with 20 and 50 μg/ml CRL-2868 exosomes or RANKL (positive control) compared to untreated cells (Fig. 7a). These data were confirmed also at protein level with an ELISA assay: treatment of Raw 264.7 with CRL-2868 exosomes (20 and 50 μg/ml for 6 days) or RANKL increased the amount of soluble MMP9 protein levels in culture medium (Fig. 7b). TRAP staining of

RAW 264.7 cells incubated with CRL-2868 exosomes and 25 ng/ml of RANKL (positive control), for 6 days, confirmed the induction of TRAP-positive multinucleate cells, compared with untreated cells (Fig. 7c). We confirmed this mechanism in a human pre-osteoclasts model, by treating human primary pre-osteoclasts cells for 4 days, with 20–50 μg/ml of CRL-2868 exosomes. The treatment of POs induced the gene expression of TRAP and MMP9 compared to untreated cells (Fig 8a). The ELISA assay for MMP9 confirmed the increased release of metalloprotease in exosome-treated human pre-osteoclasts (Fig. 8b). In order to confirm that CRL-2868 derived exosomes are enriched in AREG, and that this molecule is responsible of the observed effect, we analyzed the levels of AREG contained in conditioned media previously deprived of exosomes (CM- Exo). As showed by western blotting, CM- Exo did not contain AREG (Figure 9a). We tested the effects of CM- Exo on osteoclast differentiation and we observed that CM- Exo had not effects on RANKL at protein and mRNA levels (Figure 9b and c), MMP9 and TRAP gene expression (Figure 9d) and MMP9 at protein level (Fig.9e). These data suggest that CRL-2868 exosomal AREG induces EGFR pathway activation and and the upregulation of endogenous RANKL in osteoclast precursors, suggesting their role as osteoclastogenesis inducers. Western blotting analysis of exosomes released by other three cell lines (NSCLC: A549; Prostate cancer: PC3; Breast Cancer: MDA-MB-231) inducing bone metastases showed an exosomal enrichment of AREG compared to parental cells, supporting the potential role of exosomal AREG released by cancer cells as predictive biomarker of bone metastatic niche formation (Fig.10).

3.6 Amphiregulin contained in NSCLC-exosomes induces osteoclast differentiation

In order to further confirm that exosomal AREG induces EGFR pathway activation causing osteoclast differentiation, Raw 264.7 cells were first treated with recombinant AREG (Rec-AREG). Confocal microscopy analysis of RAW 264.7 cells, treated for 6 days with Rec-AREG showed the induction of multinucleated morphology typical of mature osteoclasts and filopodia formation (Fig 11a). Moreover, RAW 264.7 cells treatment with Rec-AREG for 6 days is able to increase the expression of the osteoclast differentiation markers (TRAP and MMP9) at mRNA and protein level compared with untreated RAW 264.7 cells (Fig. 11b-d). The osteoclast markers modulation in RAW 264.7 cells induced by Rec-AREG treatment is comparable to that achieved following CRL-2868 exosomes treatment. Moreover, the treatment of RAW 264.7 cells with Rec-AREG induced an increase of EGFR phosphorylation (Fig. 12a and b), that in turn enhanced the expression of msRANKL at mRNA and protein level (Fig. 12c and d) similar to those obtained with CRL-2868 exosomes treatment.

3.7 Erlotinib and Neutralizing antibodies revert the effects of NSCLC exosomes in osteoclast differentiation

The involvement of exosomal AREG in osteoclastogenesis regulation mediated by EGFR pathway activation was confirmed through several experiments. As first, we used Erlotinib to abrogate the effects of Rec-AREG and NSCLC-exosomes in osteoclast differentiation. Furugaki and colleagues have demonstrated that Erlotinib inhibits tumor-induced osteolytic bone metastasis by suppressing osteoclast activation through (i) the inhibition of tumor growth at the bone metastatic sites, (ii) the osteolytic factor production in tumor cells, (iii) the osteoblast proliferation and osteoclast differentiation from mouse bone marrow cells (biblio). Confocal microscopy analysis showed that co-treatment of RAW 264.7 with CRL-2868 exosomes plus Erlotinib or co-treatment of RAW 264.7 with Rec-AREG and Erlotinib abrogates the morphological differentiation of RAW 264.7 cells in mature osteoclasts induced by CRL-2868 exosomes or Rec-AREG treatment alone (Fig 11a). Moreover through qPCR analysis we demonstrated that co-treatment of RAW 264.7 with Rec-AREG and Erlotinib for 6 days decreased mRNA expression of TRAP and MMP9 compared to Rec-AREG treatment alone (Fig. 11 b). These data were confirmed also at protein level with an ELISA assay: RAW 264.7 cells co-treated for 6 days, with Rec-AREG and Erlotinib showed a decreased amount of soluble MMP9 protein levels in culture medium compared to Rec-AREG treatment (Fig. 11c). TRAP staining of RAW 264.7 cells co-treated for 6 days with Rec-AREG and Erlotinib showed a reduction of TRAP-positive multinucleate cells, compared with Rec-AREG treated cells (Fig. 11d). The role of Erlotinib in abrogating the effects of NSCLC-exosomes in osteoclast differentiation was also demonstrated by following experiments. We demonstrated through qPCR analysis that co-treatment of RAW 264.7 with CRL-2868 exosomes (20–50 μg/ml) and Erlotinib for 6 days, decreased mRNA expression of TRAP and MMP9 compared to CRL-2868 exosomal treatment alone (Fig. 13a). These data were confirmed also at protein level with an ELISA assay; RAW 264.7 cells co-treated for 6 days, with 20–50 μg/ml of CRL-2868 exosomes and Erlotinib showed a decreased amount of soluble MMP9 protein levels in culture medium compared to CRL-2868 exosomes treatment (Fig. 13b). TRAP staining of RAW 264.7 cells co-treated for 6 days, with 20–50 μg/ml of CRL-2868 exosomes and Erlotinib showed a reduction of TRAP-positive multinucleate cells, compared with CRL-2868 exosomes treated cells (Fig. 13c). As shown by western blotting analysis, in RAW 264.7 cells the co-treatment with CRL-2868 exosomes plus Erlotinib or Rec-AREG plus Erlotinib reverted the increase of EGFR phosphorylation induced by CRL-2868 exosomes or Rec-AREG treatment alone (Fig. 12a and b). The role of CRL-2868 exosomal AREG in osteoclastogenesis induction was

also confirmed by co-treatment of RAW 264.7 with CRL-2868 exosomes and AREG neutralizing antibodies. As shown in Fig. 14a, the co-treatment of RAW 264.7 with CRL-2868 exosomes and AREG neutralizing antibodies for 6 days, caused a decrease of TRAP positive multinucleate osteoclasts cells compared to the treatment with exosomes alone (Fig.14a). Through real time PCR analysis of mRNA expression of TRAP and MMP9 we demonstrated that co-treatment with CRL-2868 exosomes and AREG neutralizing antibodies reverted the effects on osteoclast differentiation mediated by exosomes treatment alone (Fig.14b). The proteic MMP9 modulation was also confirmed by an ELISA assay (Fig. 14c). These data showed that the co-treatment of RAW 264.7 with CRL-2868 exosomes and AREG neutralizing antibodies or co-treatment of RAW 264.7 with CRL-2868 exosomes and Erlotinib reverted the effects on osteoclast differentiation mediated by exosomal treatment alone, confirming the role played by AREG in osteoclast differentiation mediated by EGFR pathway activation. We obtained similar results after treatment of Raw 264.7 cells with A549 exosomes plus neutralizing antobodies for AREG and the co-treatment with A549 exosomes and Erlotinib showing the abrogating of the effects induced by A549-exosomes in osteoclast precursors differentiation (Figure 15a-c).

3.8 Knockdown of AREG in CRL-2868 cells causes a decrease of exosomal AREG

According to the results described so far, our data indicated that elevated levels of AREG in NSCLC-exosomes induce EGFR pathway activation thus promoting osteoclast differentiation. In order to confirm our hypothesis, we reduced the AREG level in the CRL-2868 cells by stably expressing human AREG shRNA plasmid. Following puromycin (4 μg/mL) selection, we isolated AREG shRNA cells (AREG-knockdown CRL-2868 cells) and compared them with cells transfected with empty vector (Mock-CRL-2868 cells) and control AREG shRNA plasmid (Scramble-CRL-2868 cells). Through real time PCR analysis of mRNA expression of AREG in CRL-2868 cells transfected with AREG shRNA plasmid (AREG-knockdown CRL-2868 cells), empty vector (Mock-CRL-2868 cells) and control AREG shRNA plasmid (Scramble-CRL-2868 cells), we observed, as expected, that the expression levels of AREG decreased in AREG shRNA cells with respect to control cells (Fig. 16a). Western blotting of AREG in AREG-knockdown CRL-2868 cells showed that also the protein expression levels of AREG decreased in AREG shRNA cells with respect to control cells (Fig.16b). We also found a strong decrease of AREG levels in CRL-2868 exosomes from AREG-knockdown CRL-2868 cells, with respect to CRL-2868 exosomes from control cells, as showed by western blotting (Fig. 16c). In RAW 264.7 cells and human pre-osteoclasts, the treatment for 6 days,

with exosomes released by AREG-knockdown CRL-2868 cells did not affect the expression of the osteoclast differentiation markers compared to CRL-2868 exosomes from control cell, as demonstrated by the levels of TRAP and MMP9 mRNA (Fig. 17a,b).Furthermore, as shown in Fig. 17c, Raw 264.7 cells treatment with exosomes released by CRL-2868 cells Control, Mock and Scramble induced the formation of TRAP-positive multinucleate cells compared to untreated RAW 264.7 cells or incubated for six days with exosomes released by AREG-knockdown CRL-2868 cells. These data confirm that the reduction of AREG level in CRL-2868 exosomes from AREG-knockdown CRL-2868 cells, impair the role of CRL-2868 exosomes in osteoclastogensis induction.

3.9 Exosomes released in plasma of NSCLC patients modulate osteoclastogenesis in human primary osteoclasts

In order to confirm *ex vivo* the effects of exosomal AREG on osteoclastogenesis, human primary osteoclasts were treated with exosomes released in plasma of NSCLC patients at different stages of disease progression, with or without bone metastases. Exosomes (30 μg) isolated from plasma (1, 5 ml) of four NSCLC patients (Pz 1: stage I, Pz 2: stage IB, Pz 3: stage IIIA, Pz 4: stage IIIA) were characterized by Western blotting, using antibodies specific for ALIX, TSG101 to confirm their exosomal identity (Fig. 18a). We demonstrated that exosomes released in plasma of twenty NSCLC patients at different disease stage contained AREG, as showed by a representative western blotting of exosomes purified from ten samples of NSCLC plasma patients at different disease stages (Fig.18b). However, despite the described correlation between increased amounts of AREG in NSCLC (123,154) sera and poor prognosis we did not find the same correlation with exosomal AREG and NSCLC stadiation. We demonstrated that exosomes released in plasma of NSCLC patients modulate osteoclastogenesis in human primary osteoclasts. Human PBMCs were treated with RANKL and dexamehasone, after 4 days, the adherent cells were mononucleated, expressed TRAP and considered as committed preosteoclast cells (POs). POs cultured in differentiation medium and incubated with exosomes from plasma of NSCLC patients, for 4 days, acquired the morphology of mature osteoclasts, as shown by TRAP staining assay (Fig. 18c). Moreover, Real Time PCR of TRAP and MMP9 mRNA expression of POs treated with NSCLC patients-exosomes showed that exosomes treatment induced an increased expression of TRAP (Fig.18d) and MMP9 at mRNA and protein levels (Fig. 19a and b). The same effects were obtained following Rec-AREG treatments of POs (Fig.18c and d; Fig.19 a and b). The effects on osteoclast differentiation mediated by NSCLC exosomes reverted after cotreatment with AREG neutralizing antibodies (Fig.18c and d; Fig.19 a and b). Overall, these data supported the hypothesis that AREG contained in NSCLC plasma patients

exosomes modulate osteoclastogenesis in human primary osteoclasts, by inducing MMP and TRAP expression, well known markers of osteoclast differentiation.

CHAPTER 4

Discussion

Non-small cell lung cancer (NSCLC) remains the leading cause of cancer-related deaths worldwide. Lung cancer induces both osteoblastic and osteolytic metastases formation being osteolytic metastases the most common in NSCLC (6,7). Bone microenvironment can promote the growth of lung cancer metastases through the interaction of metastatic cells with osteoclasts and osteoblasts thus promoting bone metastases (155,156). The unbalance between RANKL and OPG contributes to NSCLC development *in vivo* (7), in xenograft mice model has been demonstrated that RANKL overexpression promoted bone destruction and tumor growth of NSCLC cells (70). Several reports indicate that EGFR signaling is upregulated in NSCLC and in a variety of tumors metastasizing to the bone, making it an attractive molecular target for tumor treatment. Furthermore, it was demonstrated that EGFR regulates osteoclast differentiation through the crosstalk with RANK signaling (122). EGFR is expressed in osteoclast lineage cells and RANKL-mediated osteoclastogenesis requires intact EGFR signaling. Interestingly, EGFR-deficient mice showed defective osteoclast recruitment (157).

Although different therapeutic strategies, including surgery, radiation, chemotherapy, and targeted molecular therapy among which tyrosine kinase inhibitors are commonly used in lung cancer treatment, either alone or in combination, the prognosis for lung cancer is still poor, due primarily to therapeutic resistance and high metastasis rates (127). Unfortunately, to obtain a tissue sample to monitor lung cancer disease progression is still a main problem, especially during recurrence, for this reason new and non-invasive early diagnostic, predictive and prognostic biomarkers are needed (128,129). Recently, the implementation of liquid biopsies, in particular exosomes, in diagnosis, prognosis and follow-up of lung cancer patients is of great clinical interest (130,131). Exosomes have

a key role in the cell-cell communication and they have been recently indicated as important actors in metastatic niche preparation.

Our study increases the knowledge in the complex interaction between bone microenvironment and lung cancer cells by investigating the role of tumour derived exosomes. Recently our research group showed that multiple myeloma (MM) exosomes had a role in osteoclast differentiation (114). Raimondi et al., showed that exosomes released by MM cells are involved in osteoclasts differentiation. These exosomes induced the differentiation of murine RAW 264.7 and human primary preosteoclasts in mature osteoclasts, increasing the expression of osteoclast markers such as Cathepsin K (CTSK), Matrix Metalloproteinase 9 (MMP9), and Tartrate-resistant Acid Phosphatase (TRAP) (114). Considering that EGFR signalling is upregulated in NSCLC and play a central role in osteoclast differentiation regulation through the crosstalk with RANK signaling (137), we investigated in this new study the involvement of EGFR pathway in osteoclastogenesis induction mediated by cancer derived exosomes.

In this study we isolated and characterized through morphological and biochemical analyses exosomes released in CRL-2868 conditioned media (Fig.1) and in plasma of NSCLC patients (Fig.19). In line with data from literature, we showed that RAW 264.7 cells treated with NSCLC exosomes activate EGFR pathway that caused an upregulation of RANKL (Fig.6) and of osteoclastogenesis markers (MMP9 and TRAP) (Fig.7,8). In order to confirm the central role of EGFR pathway activation in the induction of osteoclastogesis, we tested the effects of Erlotinib in the osteoclasts differentiation mediated by NSCLC exosomes. Tyrosine kinase inhibitors (TKIs) of EGFR activity have been introduced several years ago to treat NSCLC patients. Erlotinib, one of the first-generation EGFR-TKIs (27,28) binds competitively and reversibly to the ATP-binding site of the EGFR TK domain, and shows a significant advance treatment in selected NSCLC patients with activating EGFR mutations. Our experiments demonstrated that the co-treatment of pre-osteoclasts with exosomes and Erlotinib reverted the effect of exosomes (Fig.11,12,13) in osteoclasts differentiation, indicating that the block of EGFR pathway inhibited osteoclastogenesis.

Of the family of seven peptide growth factors that bound and activated EGFR, we focused on Amphiregulin as the main exosomal actor involved in the induction of osteoclastogenesis mediated by EGFR pathway activation. Data in literature reported that this protein is overexpressed in several cancers such as colon, breast and lung (122). Moreover, it has been described that exosomes contain EGFR ligands, among which Amphiregulin (AREG). Our research group had previously demonstrated that leukaemic cell (LAMA84) and blood samples of CML patient's exosomes contain AREG, and are able to activate EGFR signalling in bone marrow stromal cells (HS5), increasing the expression of SNAIL and its targets, MMPs and IL8 (121). Higginbotham et al., showed that AREG

is released in extracellular vescicles released from HCA-7 colorectal cells; data from the same paper showed that treatment with exosomes released from AREG-expressing MDCK (Madin-Darby canine kidney) cells induce the highest invasive activity in MDA-MB-231-derived LM2-4175 and LMO-1833 recipient cells that metastasize to lung and bone, respectively, compared to exosomes released from TGF-α or HB-EGF-expresing MDCK cells (120). Moreover, Chang et al., demonstrated that AREG levels in plasma of NSCLC patients correlate with poor prognosis (123). In order to test if exosomal AREG was an important molecule in the induction of EGFR pathway, we performed experiments with recombinant AREG and AREG neutralizing antibody. As showed in Fig.11 and Fig.12, the treatment of pre-osteoclasts with recombinant AREG had the similar effects of NSCLC-exosomes on the induction of EGFR phosphorylation causing an increase of RANKL that modulated MMP9 and TRAP expression and induced the typical phenotype of mature osteoclasts. The co-treatment of pre-osteoclasts with NSCLC-exosomes and AREG neutralizing antibodies reverted the effects of osteoclasts differentiation mediated by NSCLC exosomes (Fig.14,15). The central role of exosomal AREG in osteoclast differentiation was confirmed by the knockdown of AREG in CRL-2868 cells. The decrease of AREG levels in CRL-2868 cells inhibited the accumulation of this molecule into exosomes, reverting the effects on osteoclastogenesis induced by lung cancer exosomes (Fig.16,17). The data obtained in Raw 264.7 cells treated with exosomes released by CRL-2868 cell line were confirmed with human committed preosteoclast PMBCs treated with esosomes isolated from plasma of twenty NSCLC patients at different disease stages. We demonstrated that NSCLC patient exosomes were enriched in AREG and they induced the human preosteoclast differentiation in mature osteoclasts. These effects reverted after treatment with AREG neutralizing antibodies (Fig.18,19). However, despite described correlation between increased amounts of AREG in NSCLC (123,154) sera with poor prognosis we did not find the same correlation with exosomal AREG and NSCLC stadiation. Probably, constitutive EGFR activation in NSCLC cells leads to an increase of AREG signaling since the early disease stage, driving the cancer progression toward osteolytic bone metastasis.

Taken together our data indicated that exosomal AREG induces the activation of EGFR pathway that increases, in pre-osteoclasts treated with NSCLC-exosomes, the expression of RANKL at mRNA and protein levels. RANKL, in turn is able to induce the expression of proteolytic enzymes considered osteoclastogenesis markers, triggering the vicious cycle.

We demonstrated for the first time the role of AREG contained in NSCLC-exosomes in the osteoclast differentiation, providing the basis for further studies to develop new therapeutic strategy to inhibit the fatal attraction between lung cancer and bone in order to enhance NSCLC patients outcome.

CHAPTER 5

Figures and Tables

5.1 Characterization of exosomes released by NSCLC cells

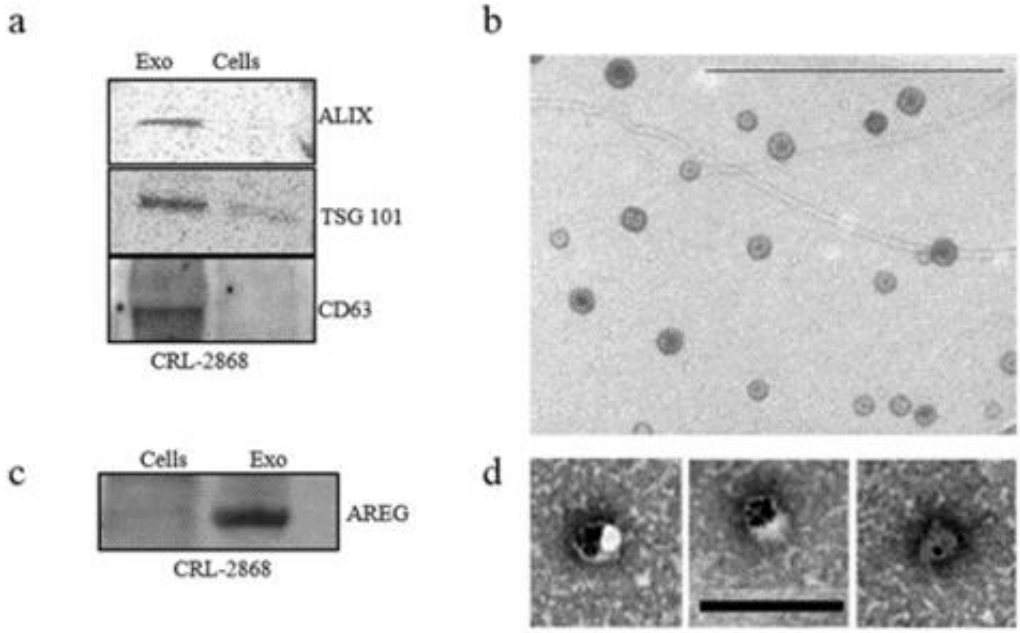

Figure 1: (**a**) Detection by western blotting of ALIX, TSG 101 and CD63 in 30 µg of exosomes purified conditioned medium of CRL-2868 cells compared to 30 µg of parental cells whole lysate. (**b**) Representative negative staining EM image of exosomes released by CRL-2868 cells. Scale bar 500 nm. (**c**) Detection by western blotting of AREG in 30 µg of CRL-2868 exosomes compared to 30 µg of parental cells whole lysate. (**d**) Gold labelling immune-electron microscopy and negative staining indicating the presence of AREG antigen on exosomes. Scale bar 200 nm.

5.2 CRL-2868 exosomes are internalized by RAW 264.7 cells and induce preosteoclasts morphological differentiation

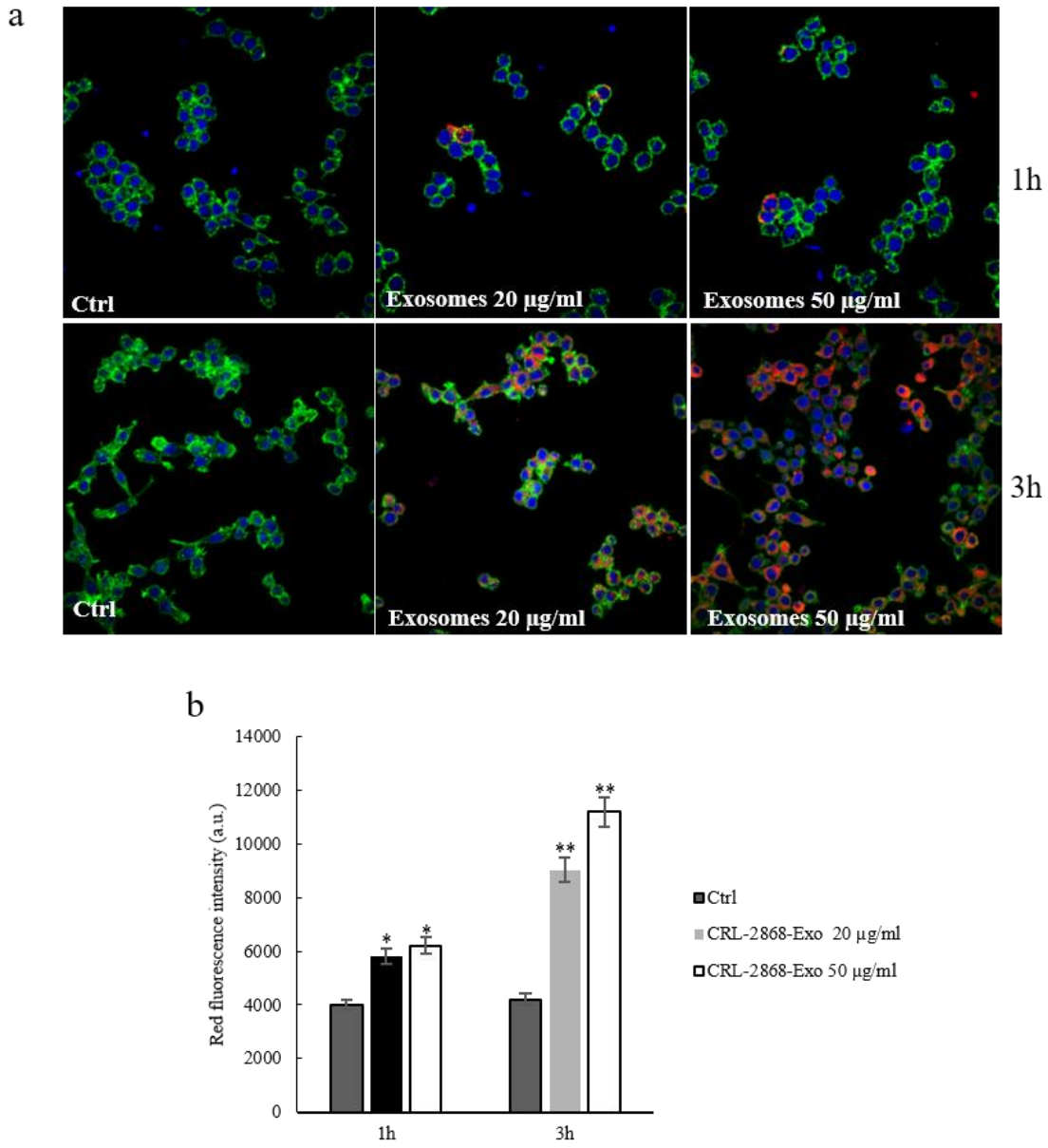

Figure 2: (a) Confocal microscopy analysis of RAW 264.7 cells treated, for 1 and 3 hours, with 20 µg/ml (Exosomes 20 µg/ml) and 50 µg/ml (Exosomes 50 µg/ml) of CRL-2868 exosomes, compared to untreated RAW 264.7 cells (Ctrl). RAW 264.7 were stained with ActinGreen (green), nuclear counterstaining was performed using Hoescht (blue); exosomes were labelled with PKH26 (red). Scale bar 50 µm. (**b**) Semi-quantitative analysis of CRL-2868 exosomes internalization, measured as red fluorescence intensity in the cytoplasm of RAW 264.7 cells.

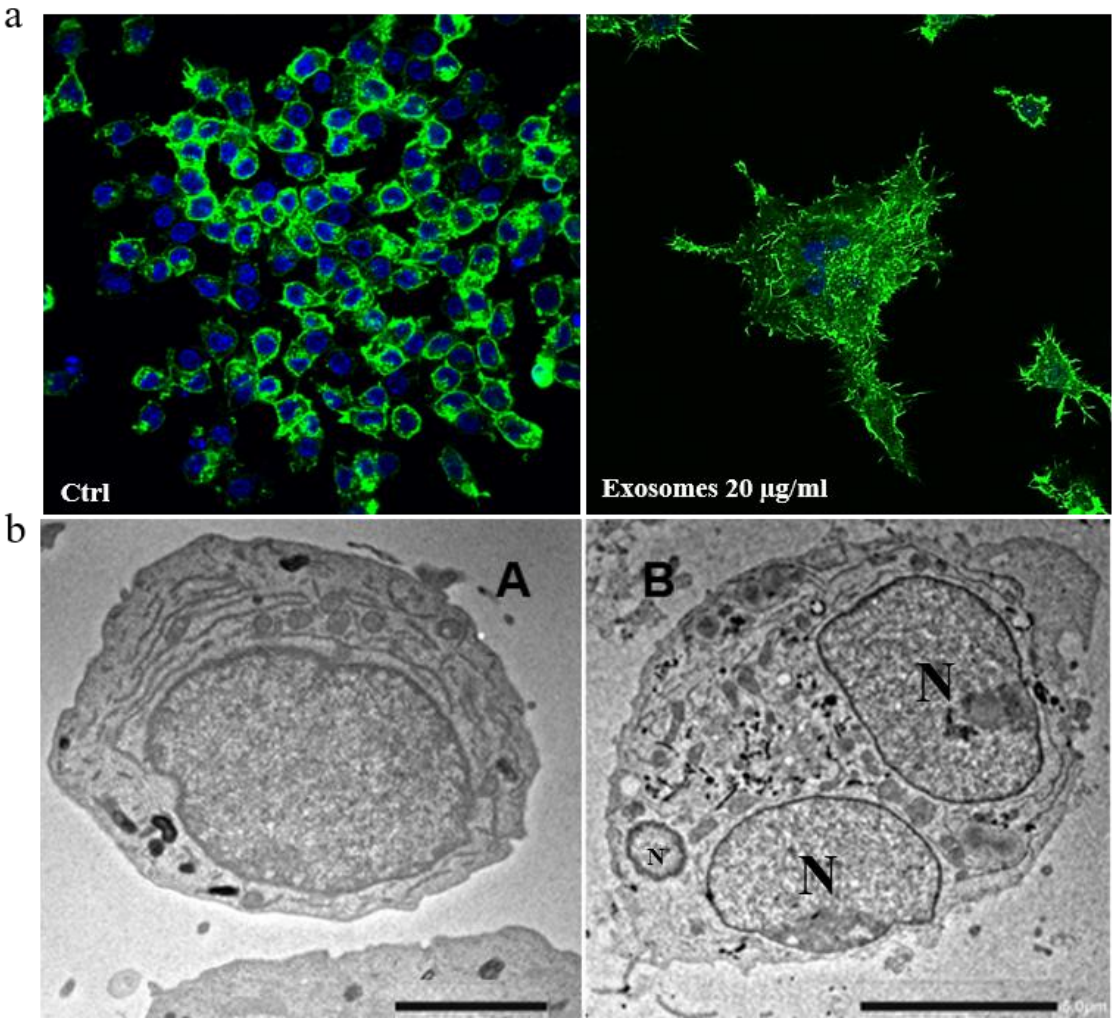

Figure 3: (a) Confocal microscopy analysis of RAW 264.7 cells treated, for 6 days with 20 µg/ml (Exosomes 20 µg/ml) of CRL-2868 exosomes, compared to untreated RAW 264.7 cells (Ctrl). Scale bar 10 µm. (**b**) Comparative morphological features of pre-osteoclasts grown in the absence (A) and presence (B) of CRL-2868 exosomes and analyzed by TEM. Scale bars: A = 2 µm; B = 5 µm.

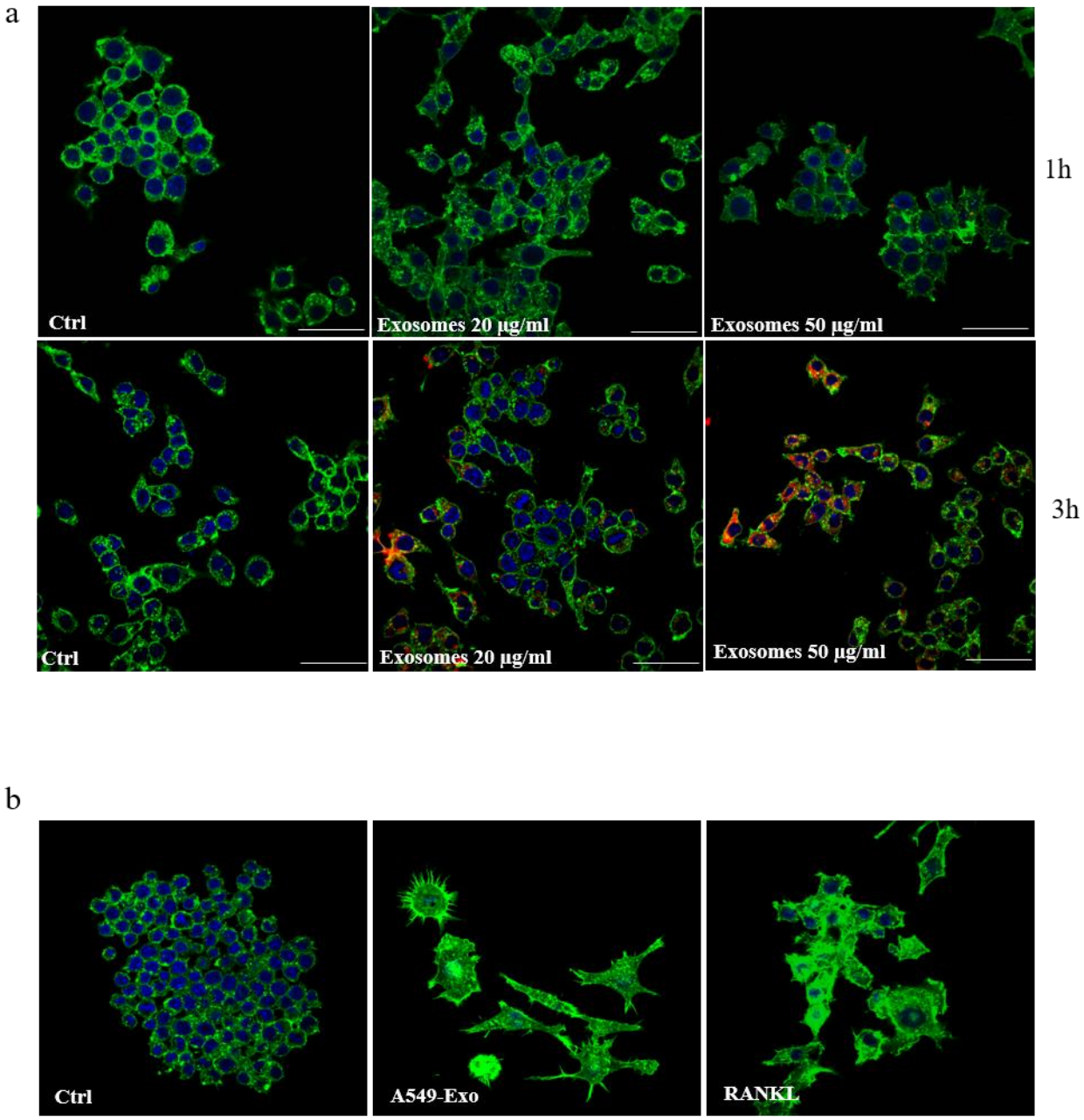

Figure 4: (a) Confocal microscopy analysis of RAW 264.7 cells treated, for 1 and 3 hours, with 20 µg/ml (Exosomes 20 µg/ml) and 50 µg/ml (Exosomes 50 µg/ml) of A549 exosomes, compared to untreated RAW 264.7 cells (Ctrl). RAW 264.7 were stained with ActinGreen (green), nuclear counterstaining was performed using Hoescht (blue); exosomes were labelled with PKH26 (red). **(b)** Confocal microscopy analysis of RAW 264.7 cells treated, for 6 days with: A549 exosomes and RANKL compared with RAW 264.7 control (Ctrl). Scale bar 10 µm.

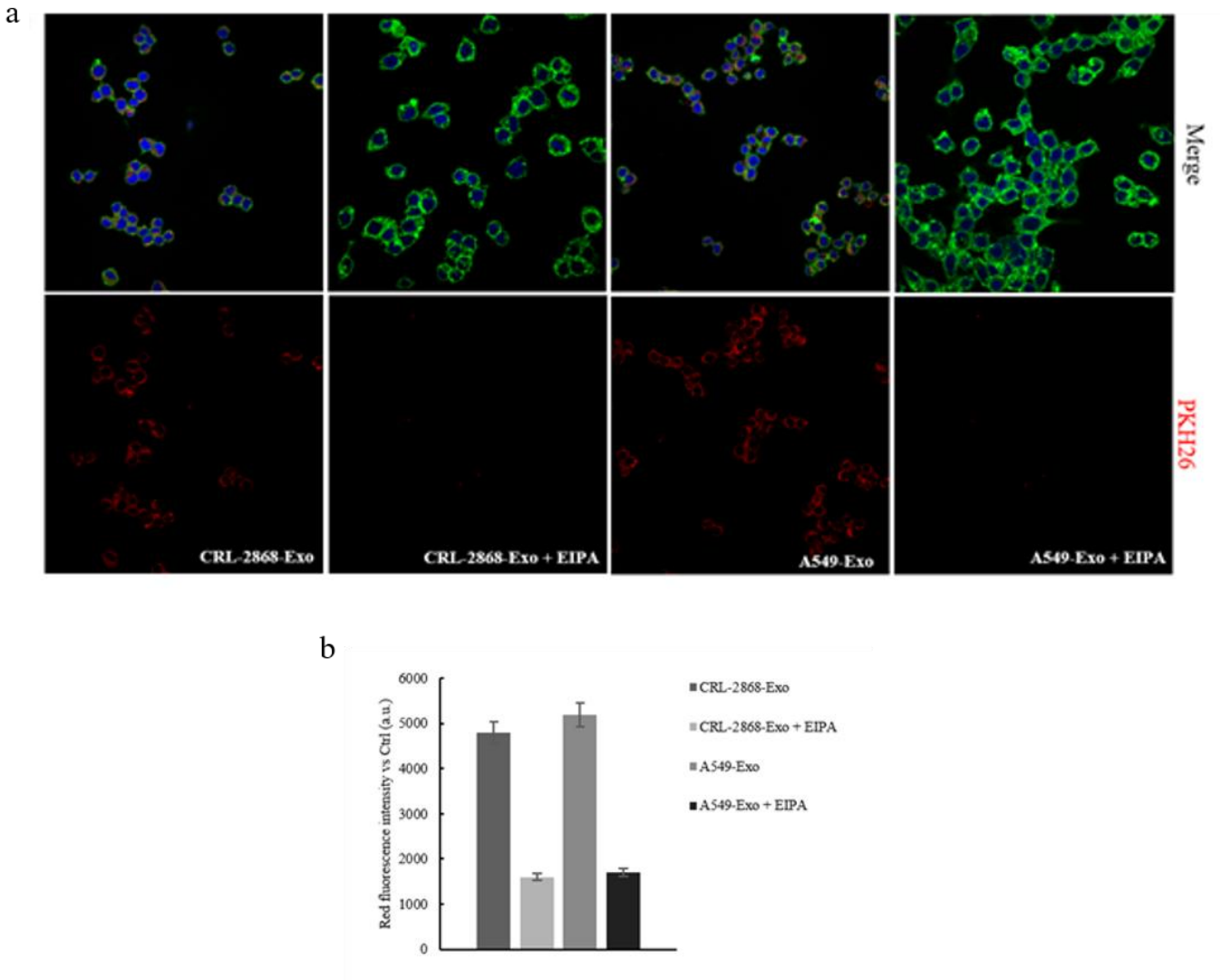

Figure 5: (a) Analysis at confocal microscopy of RAW 264.7 cells co- treated, for 3 hour, with 50 µg/ml of CRL-2868 (CRL-2868-Exo + EIPA) and A549 exosomes (A549-Exo + EIPA) plus EIPA (50 µM), compared with RAW 264.7 cells treated, for 3 hour, with 50 µg/ml of CRL-2868 (CRL-2868-Exo) and A549 exosomes (A549-Exo). Scale bar = 10 µm. **(b)** Semi-quantitative analysis of CRL-2868 exosomes internalization, measured as red fluorescence intensity in the cytoplasm of RAW 264.7 cells, after treatment with EIPA

5.3 CRL-2868 exosomes induce the activation of EGFR pathway

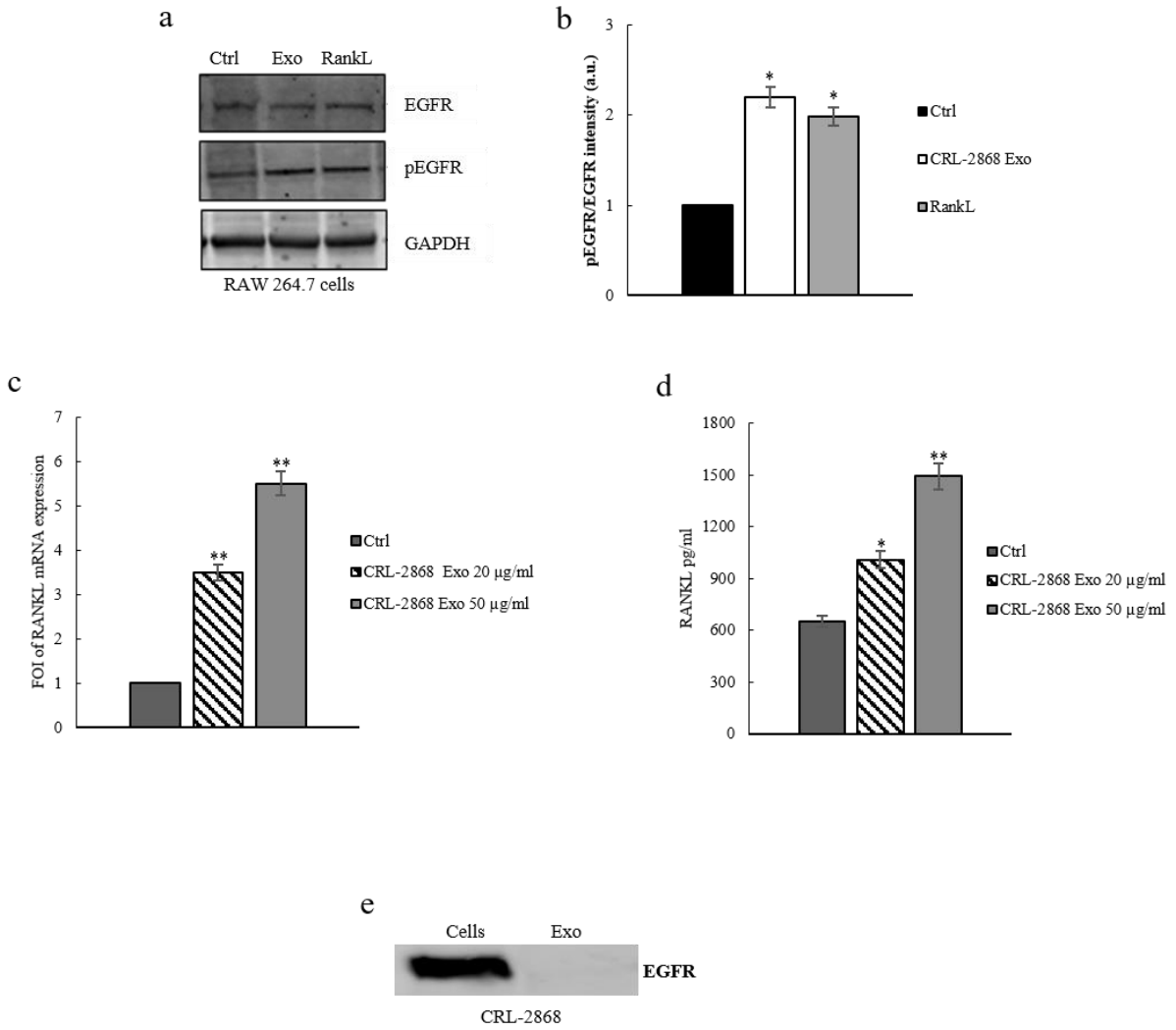

Figure 6: (**a**) Western blotting analysis of pEGFR and EGFR in whole lysate of RAW 264.7 cells treated, for 6 days, with 20 µg/ml CRL-2868 exosomes (Exo) and RANKL (positive control) compared to untreated cells (Ctrl). GAPDH was used as loading control. (**b**) Densitometric analysis of Western blotting for pEGFR/EGRF. (**c**) Evaluation by quantitative Real Time PCR of mRNA RANKL expression in RAW 264.7 cells treated, for 6 days, with 20 and 50 µg/ml CRL-2868 exosomes. (**d**) msRANKL protein levels assessed by ELISA, in RAW 264.7 cells treated, for 6 days, with 20 and 50 µg/ml CRL-2868 exosomes. (**e**) Western blot analysis of EGFR in 30µg of CRL-2868 exosomes compared to 30µg whole lysate of parental cells.

5.4 CRL-2868 exosomes induce osteoclast differentiation markers expression in RAW 264.7 cell line

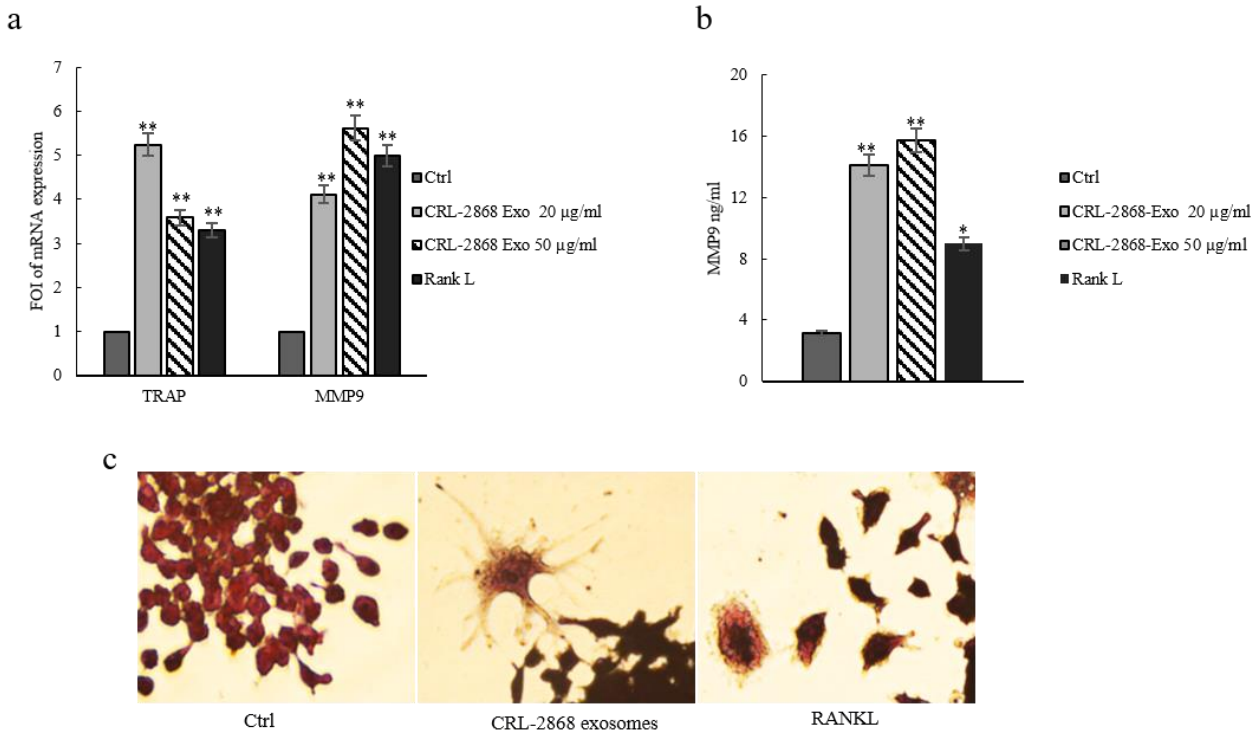

Figure 7: (a) Evaluation by quantitative Real Time PCR of mRNA expression of TRAP and MMP9 in RAW 264.7 cells treated, for 6 days, with 20–50 µg/ml CRL-2868 exosomes and RANKL (positive control). (**b**) MMP9 protein level assessed by ELISA, in RAW 264.7 cells treated, for 6 days, with 20–50 µg/ml CRL-2868 exosomes and RANKL. Values are the mean ± SD of 3 three independent experiments *$p \leq 0.05$, **$p \leq 0.01$. (**c**) TRAP staining of RAW 264.7 cells incubated with CRL-2868 exosomes and 25 ng/ml of RANKL (positive control), for 6 days, compared with untreated cells. Scale bar 10 µm.

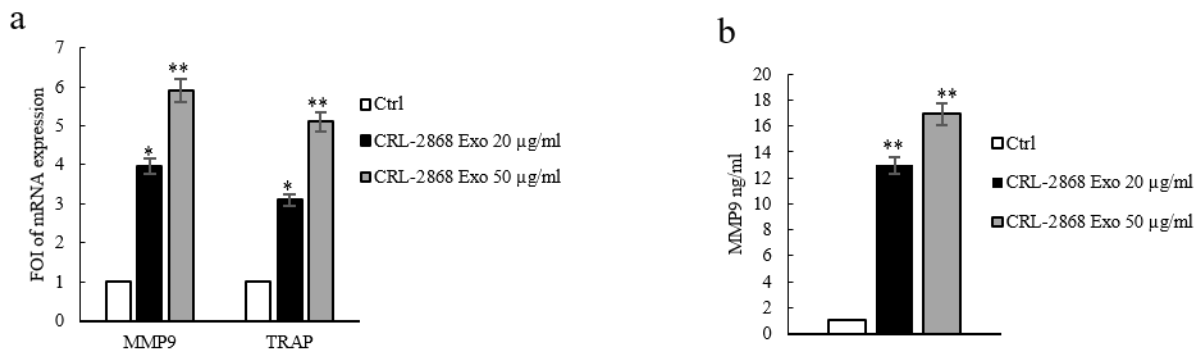

Figure 8: (**a**) Evaluation by quantitative Real Time PCR of mRNA expression of TRAP and MMP9 in human primary pre-osteoclasts treated, for 4 days, with 20–50 µg/ml of CRL-2868 exosomes. (**b**) MMP9 protein levels assessed by ELISA, in human primary pre-osteoclasts treated, for 4 days, with 20–50 µg/ml CRL-2868 exosomes. Values are the mean ± SD of three independent experiments *$p \leq 0.05$, **$p \leq 0.01$.

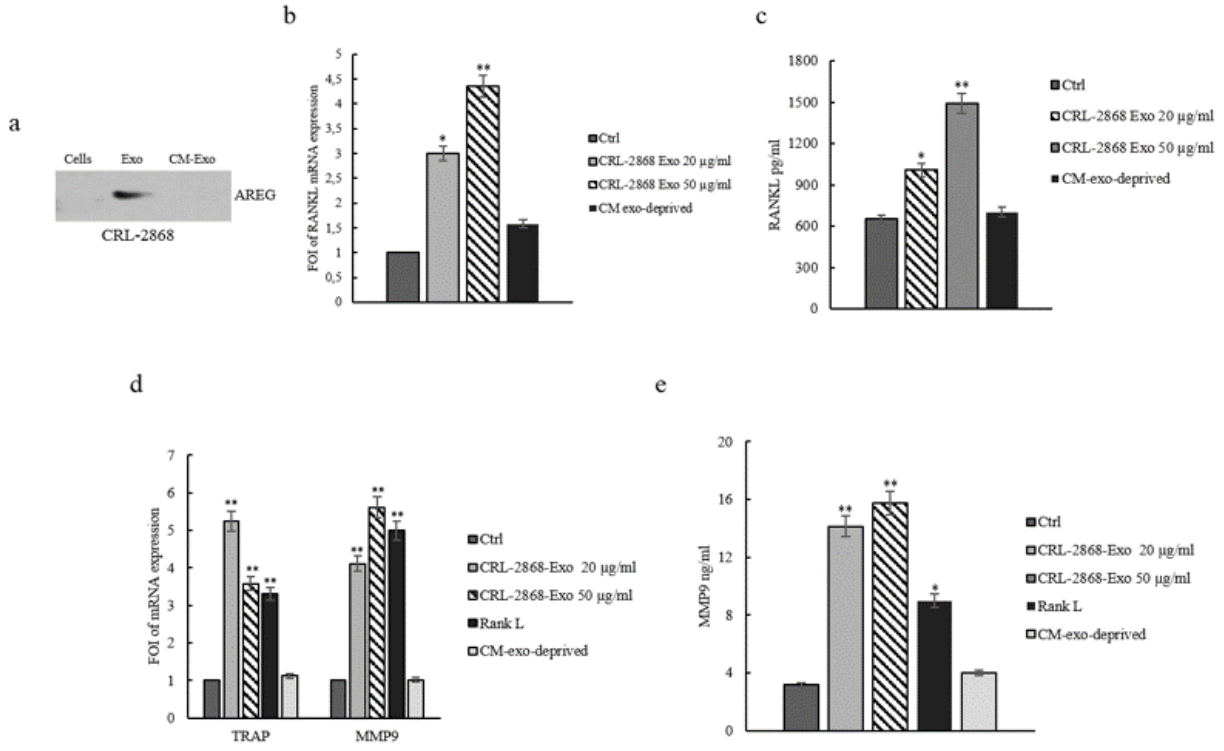

Figure 9: (a) Detection by western blotting of AREG in 30 µg of CRL-2868 exosomes (Exo) compared to 30 µg of parental cells whole lysate (Cells) and exosomes-deprived conditioned medium (CM-exo: 10 ml of medium concentrated from which 30 µg of CRL-2868 exosomes were isolated). (**b)** Evaluation by quantitative Real Time PCR of mRNA RANKL expression in RAW 264.7 cells treated, for 6 days, with 20 and 50 µg/ml CRL-2868 exosomes and exosomes-deprived conditioned medium (CM-exo). (**c)** msRANKL protein levels assessed by ELISA, in RAW 264.7 cells treated, for 6 days, with 20 and 50 µg/ml CRL-2868 exosomes and conditioned medium exosomes-deprived (CM-exo). (**d)** Evaluation by quantitative Real Time PCR of mRNA expression of TRAP and MMP9 in RAW 264.7 cells treated, for 6 days, with 20-50 µg/ml CRL-2868 exosomes, RANKL (positive control) and exosomes-deprived conditioned medium (CM-exo). (**e)** MMP9 protein level assessed by ELISA, in RAW 264.7 cells treated, for 6 days, with 20-50 µg/ml CRL-2868 exosomes, RANKL exosomes-deprived conditioned medium (CM-exo). Values are the mean ± SD of 3 three independent experiments *p≤ 0.05, **p≤ 0.01.

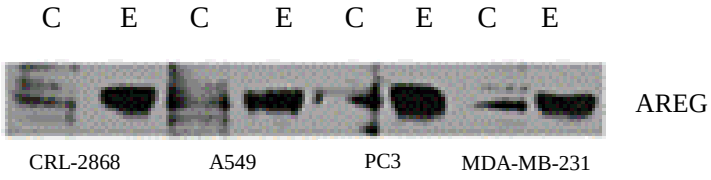

Figure 10: Detection by western blotting of AREG in 30 µg of CRL-2868, A549, PC3 and MDA-MB-231 exosomes compared to 30 µg of parental cells whole lysate.

5.5 Amphiregulin contained in NSCLC-exosomes induces osteoclast differentiation

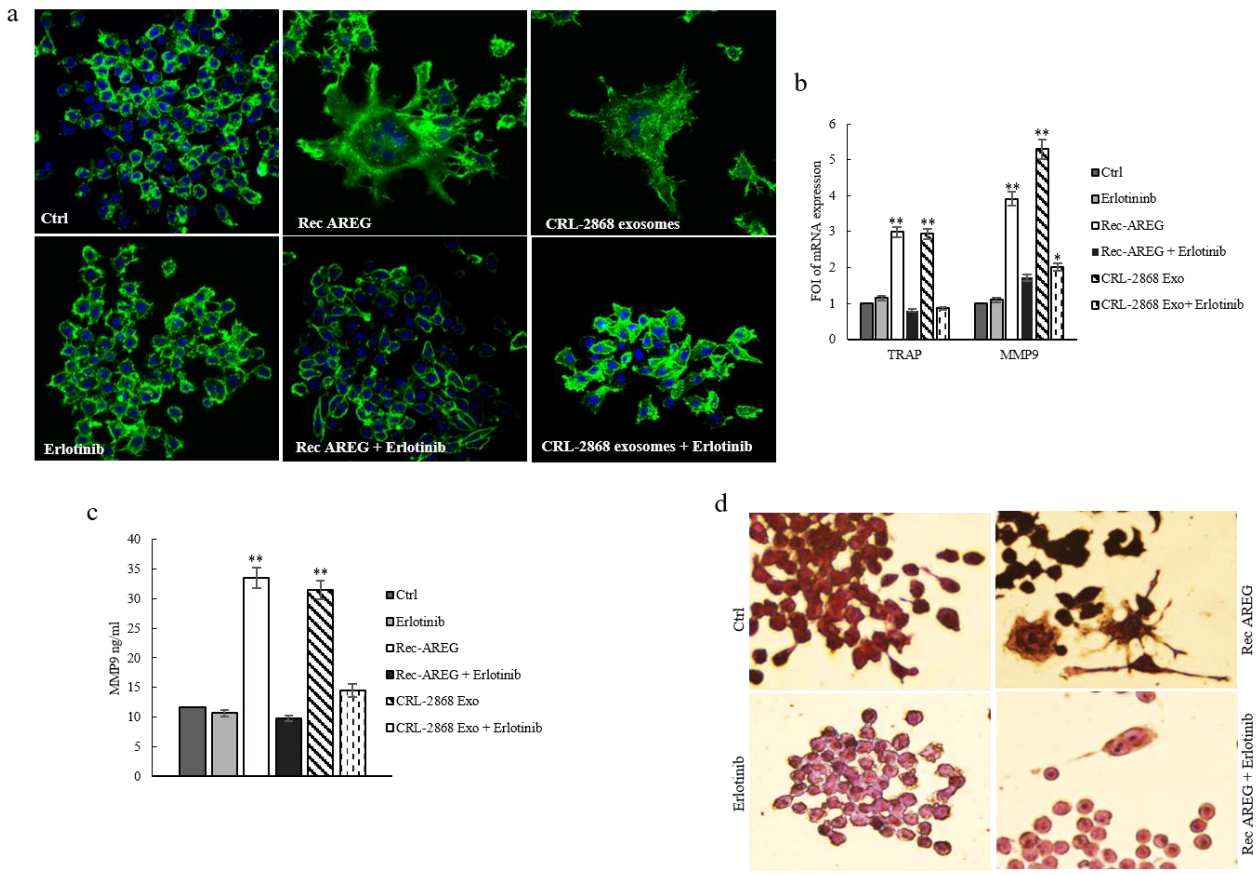

Figure 11: (**a**) Confocal microscopy analysis of RAW 264.7 cells treated, for 6 days with: CRL-2868 exosomes, CRL-2868 plus Erlotinib, Rec-AREG, Rec-AREG plus Erlotinib (Rec-AREG + Erlotinib), Erlotinib compared with untreated RAW 264.7 cells (Ctrl). Scale bar 10 µm. (**b**) Evaluation by quantitative Real Time PCR of mRNA expression of TRAP and MMP9 in RAW 264.7 cells treated, for 6 days, with: CRL-2868 exosomes, CRL-2868 exosomes plus Erlotinib (CRL-2868 Exo + Erlotinib), Rec-AREG and Rec-AREG plus Erlotinib (Rec-AREG + Erlotinib). (**c**) MMP9 protein level assessed by ELISA, in RAW 264.7 cells treated, for 6 days, with: CRL-2868 exosomes, Rec-AREG, CRL-2868 exosomes plus Erlotinib (CRL-2868 Exo + Erlotinib), Rec-AREG plus Erlotinib (Rec-AREG + Erlotinib). Values are the mean ± SD of three independent experiments *$p \leq 0.05$, **$p \leq 0.01$. (**d**) TRAP staining of RAW 264.7 cells incubated with: Rec-AREG, Erlotinib, Rec-AREG plus Erlotinib (Rec-AREG + Erlotinib), for 6 days, compared with untreated RAW 264.7 cells.

5.6 Erlotinib and Neutralizing antibodies revert the effects of NSCLC exosomes in osteoclast differentiation

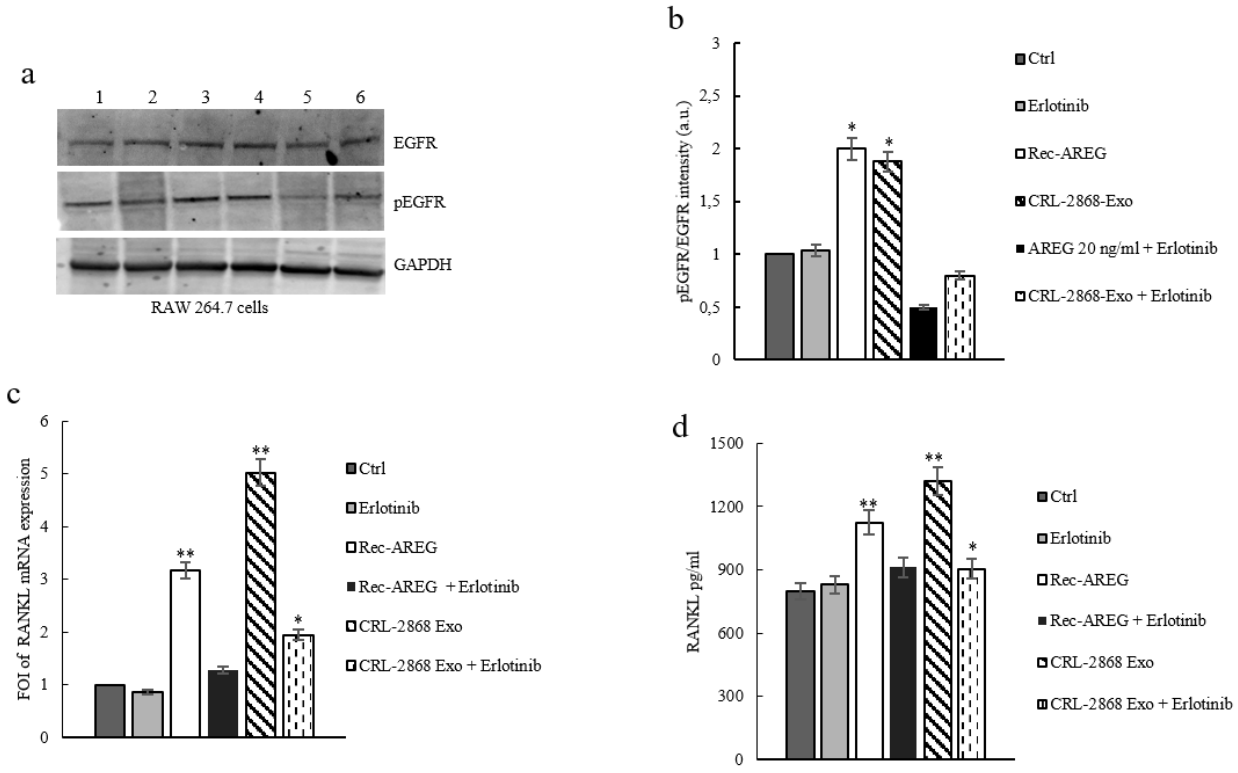

Figure 12: (**a**) Western blotting analysis of pEGFR and EGFR in whole lysate of RAW 264.7 cells treated, for 6 days, with: Erlotinib (2), Rec-AREG (3), CRL-2868 exosomes (4), Rec-AREG plus Erlotinib (5), CRL-2868 exosomes plus Erlotinib (6) compared to untreated cells (1). GAPDH was used as loading control. (**b**) Densitometric analysis of Western blotting for pEGFR/EGRF (**c**) Evaluation by quantitative Real Time PCR of mRNA expression of mRNA RANKL expression in RAW 264.7 cells treated, for 6 days, with: CRL-2868 exosomes, Rec-AREG, CRL-2868 exosomes plus Erlotinib (CRL-2868 Exo + Erlotinib), Rec-AREG plus Erlotinib (Rec-AREG + Erlotinib). (**d**) RANKL protein levels assessed by ELISA, in RAW 264.7 cells treated, for 6 days, with: CRL-2868 exosomes, Rec-AREG, CRL-2868 exosomes plus Erlotinib (CRL-2868 Exo + Erlotinib), Rec-AREG plus Erlotinib (Rec-AREG + Erlotinib). Values are the mean ± SD of 3 three independent experiments *$p \leq 0.05$, **$p \leq 0.01$.

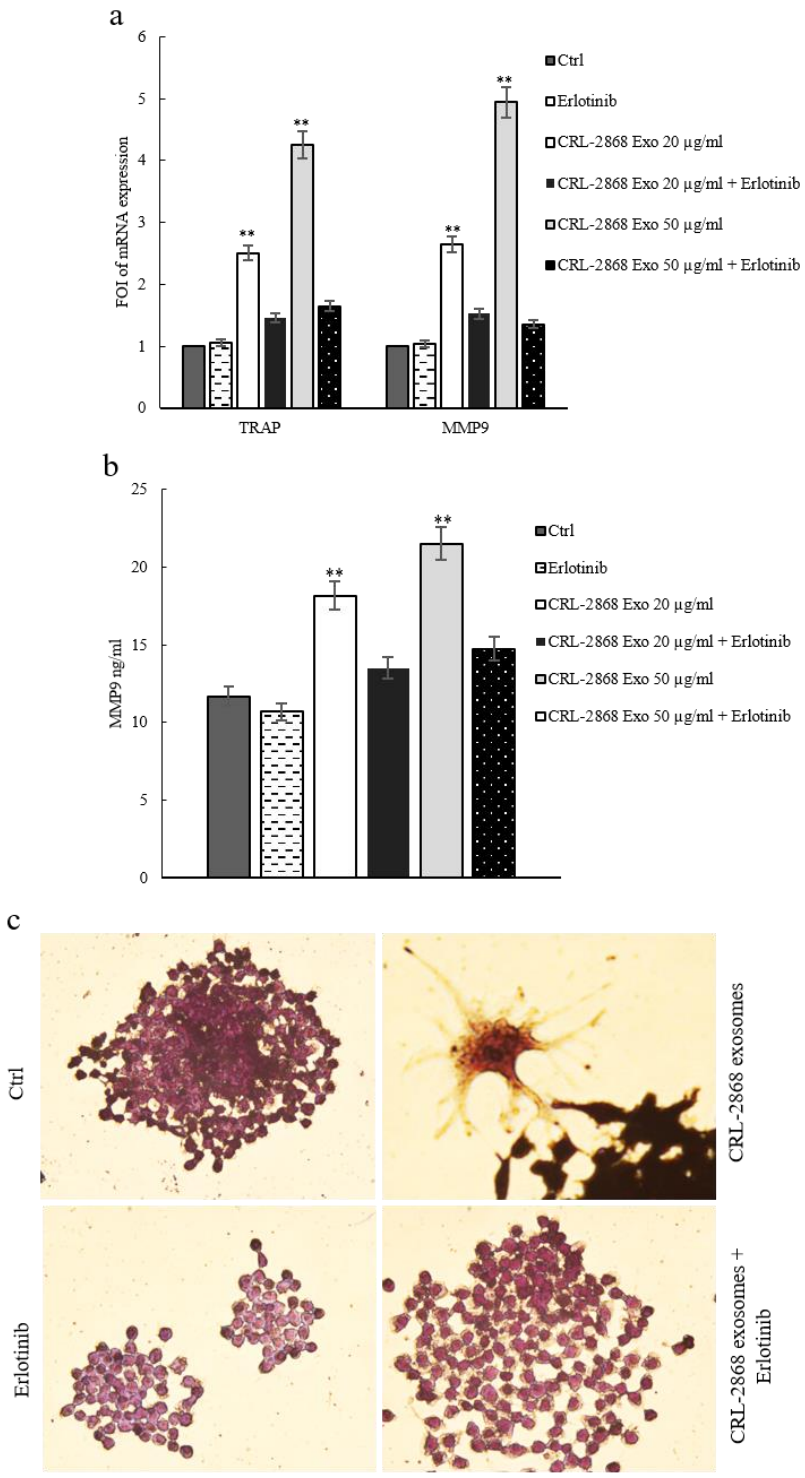

Figure 13: (a) Evaluation by quantitative Real Time PCR of mRNA expression of TRAP and MMP9 in RAW 264.7 cells treated, for 6 days, with: 20–50 µg/ml of CRL-2868 exosomes, Erlotinib and CRL-2868 exosomes plus Erlotinib. (**b**) MMP9 protein levels assessed by ELISA, in RAW 264.7 cells treated, for 6 days, with: 20–50 µg/ml of CRL-2868 exosomes, Erlotinib and CRL-2868 exosomes plus Erlotinib. Values are the mean ± SD of three independent experiments *$p \leq 0.05$, **$p \leq 0.01$. (**c**) TRAP staining of RAW 264.7 cells incubated with: CRL-2868 exosomes, Erlotinib, and CRL-2868 exosomes plus Erlotinib, for six days, compared with untreated RAW 264.7 cells. Scale bar 10 µm.

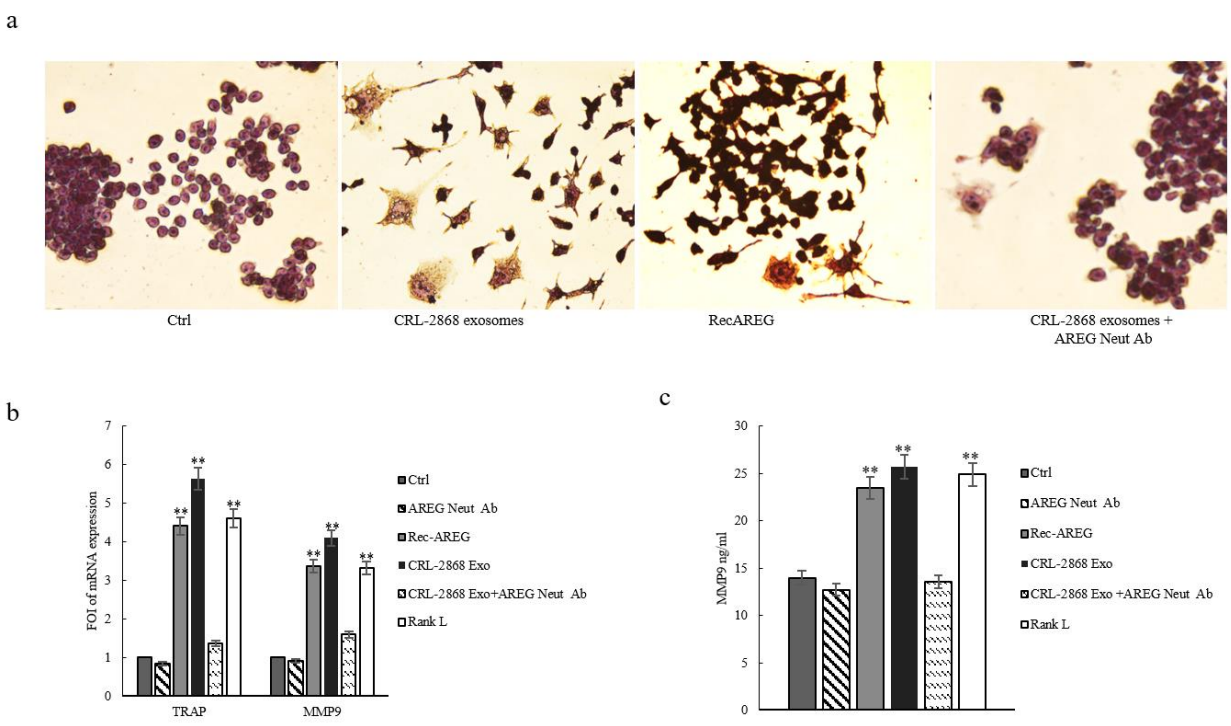

Figure 14: (**a**) TRAP staining of RAW 264.7 cells incubated with: CRL-2868 exosomes, Rec-AREG, CRL-2868 exosomes plus AREG neutralizing antibodies, for 6 days, stained for TRAP and compared with untreated cells (Ctrl). Scale bar 10 µm. (**b**) Evaluation by real Time PCR analysis of mRNA expression of TRAP and MMP9 in RAW 264.7 cells treated, for 6 days, with: CRL-2868 exosomes, Rec-AREG, AREG neutralizing antibodies, RANKL, CRL-2868 exosomes plus AREG neutralizing antibodies. (**c**) MMP9 protein levels assessed by ELISA, in RAW 264.7 cells treated, for 6 days, with: CRL-2868 exosomes, Rec-AREG, AREG neutralizing antibodies, RANKL, CRL-2868 exosomes plus AREG neutralizing antibodies. Values are the mean ± SD of three independent experiments *$p \leq 0.05$, **$p \leq 0.01$.

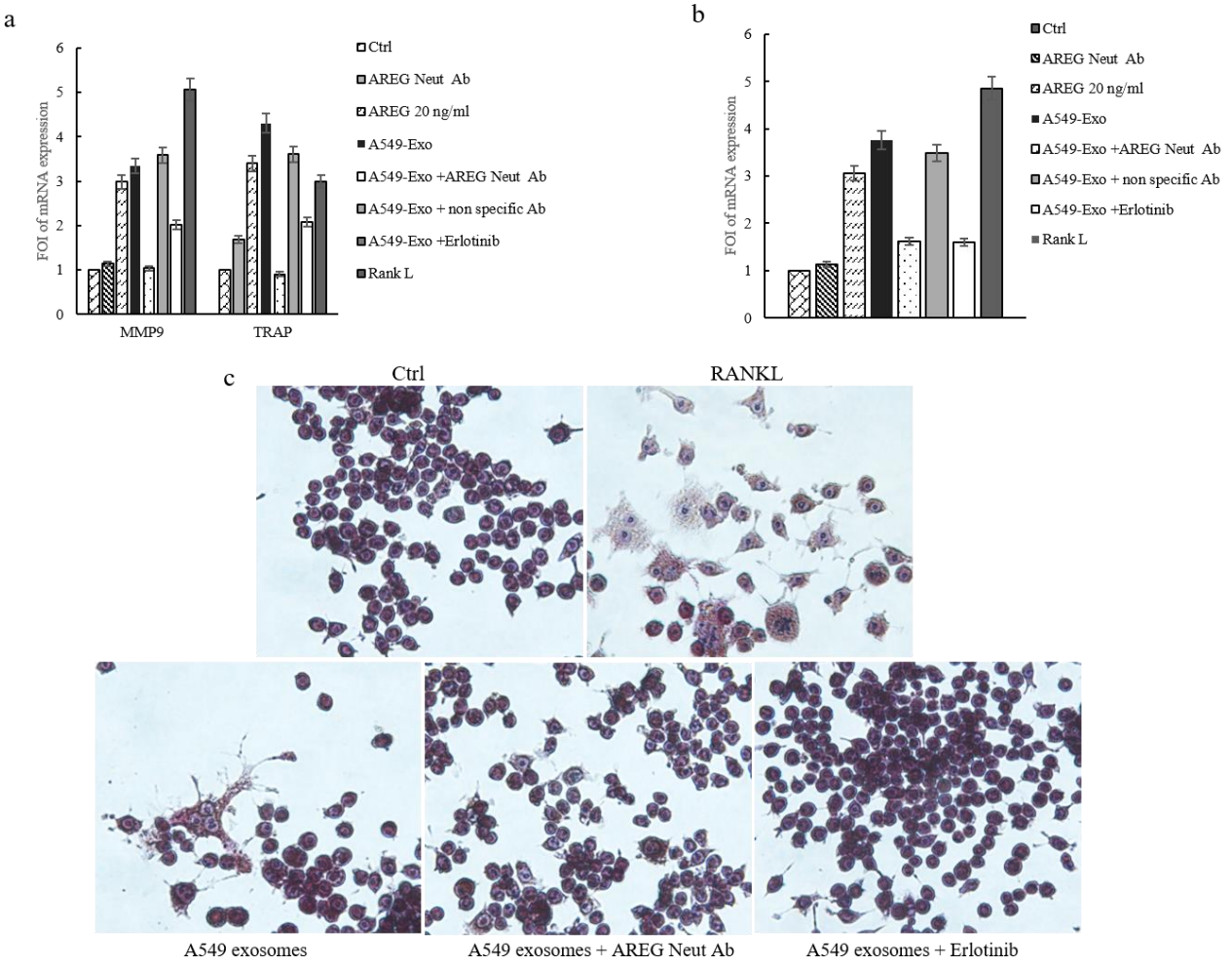

Figure 15: (**a**) Evaluation by real Time PCR analysis of mRNA expression of TRAP and MMP9 in RAW 264.7 cells treated, for 6 days, with: AREG neutralizing antibodies, Rec-AREG (20 ng/ml), A549 exosomes, A549 exosomes plus AREG neutralizing antibodies, A549 exosomes plus isotype control antibodies, A549 exosomes plus Erlotinib and RANKL. Values are the mean ± SD of 3 three independent experiments *p≤ 0.05, **p≤ 0.01. (**b**) Evaluation by real Time PCR analysis of mRNA expression of RANKL in RAW 264.7 cells treated, for 6 days, with: AREG neutralizing antibodies, Rec-AREG (20 ng/ml), A549 exosomes, A549 exosomes plus AREG neutralizing antibodies, A549 exosomes plus isotype control antibodies and A549 exosomes plus Erlotinib. (**c)** TRAP staining of RAW 264.7 cells incubated with: A549 exosomes, RANKL, A549 exosomes plus AREG neutralizing antibodies, A549 exosomes plus Erlotinib, for 6 days, stained for TRAP and compared with untreated cells (Ctrl). Scale bar 10 μm.

5.7 Knockdown of AREG in CRL-2868 cells causes a decrease of exosomal AREG

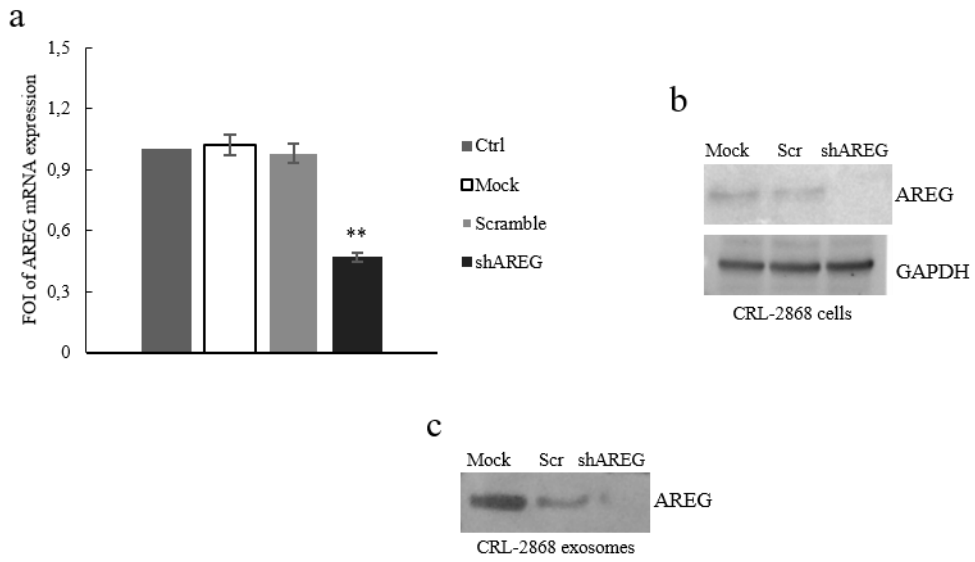

Figure 16: (**a**) Evaluation by real time PCR analysis of mRNA expression of AREG in CRL-2868 cells transfected with AREG shRNA plasmid (AREG-knockdown CRL-2868 cells), empty vector (Mock-CRL-2868 cells) and control AREG shRNA plasmid (Scramble-CRL-2868 cells). (**b**) Western blotting of AREG in whole lysate of Mock, Scramble, and AREG-knockdown CRL-2868 cells. (**c**) Western blotting of AREG in exosomes released by Mock, Scramble, and AREG-knockdown CRL-2868 cells.

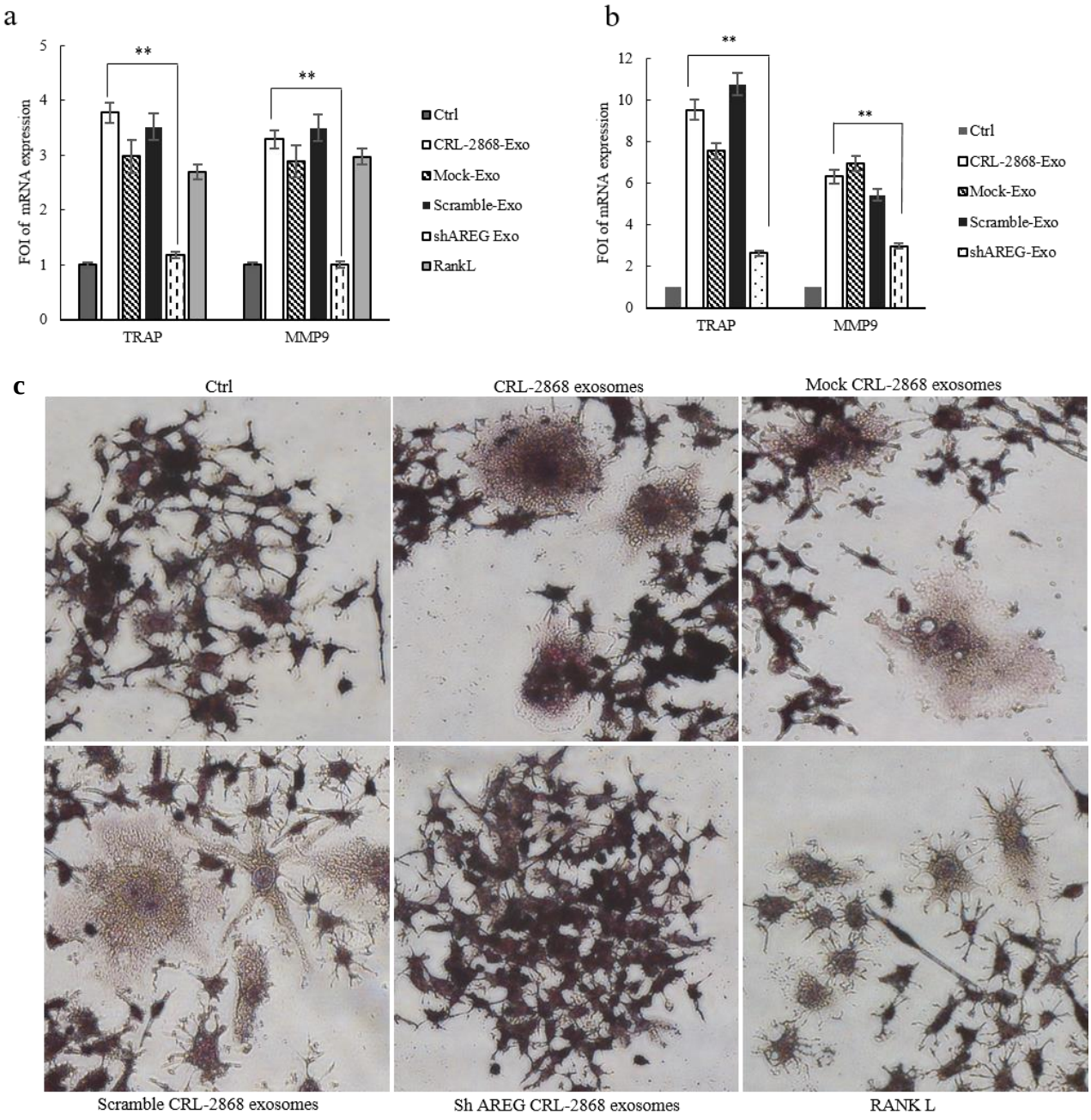

Figure 17: (**a**) Evaluation by real time PCR analysis of mRNA expression of TRAP and MMP9 in RAW 264.7 cells treated, for 6 days, with exosomes released by Control, Mock, Scramble, and AREG-knockdown CRL-2868 cells and RANKL. Values are the mean ± SD of three independent experiments *$p \leq 0.05$, **$p \leq 0.01$. (**b**) Evaluation by real time PCR analysis of mRNA expression of TRAP and MMP9 in primary human pre-osteoclasts treated for 4 days with: exosomes released by Control, Mock, Scramble, and AREG-knockdown CRL-2868 cells. Values are the mean ± SD of three independent experiments *$p \leq 0.05$, **$p \leq 0.01$. (**c**) RAW 264.7 cells were incubated with exosomes released by Control, Mock, Scramble, and AREG-knockdown CRL-2868 cells and RANKL, for 6 days, stained for TRAP and compared with untreated cells (Ctrl).

5.8 Exosomes released in plasma of NSCLC patients modulate osteoclastogenesis in human primary osteoclasts

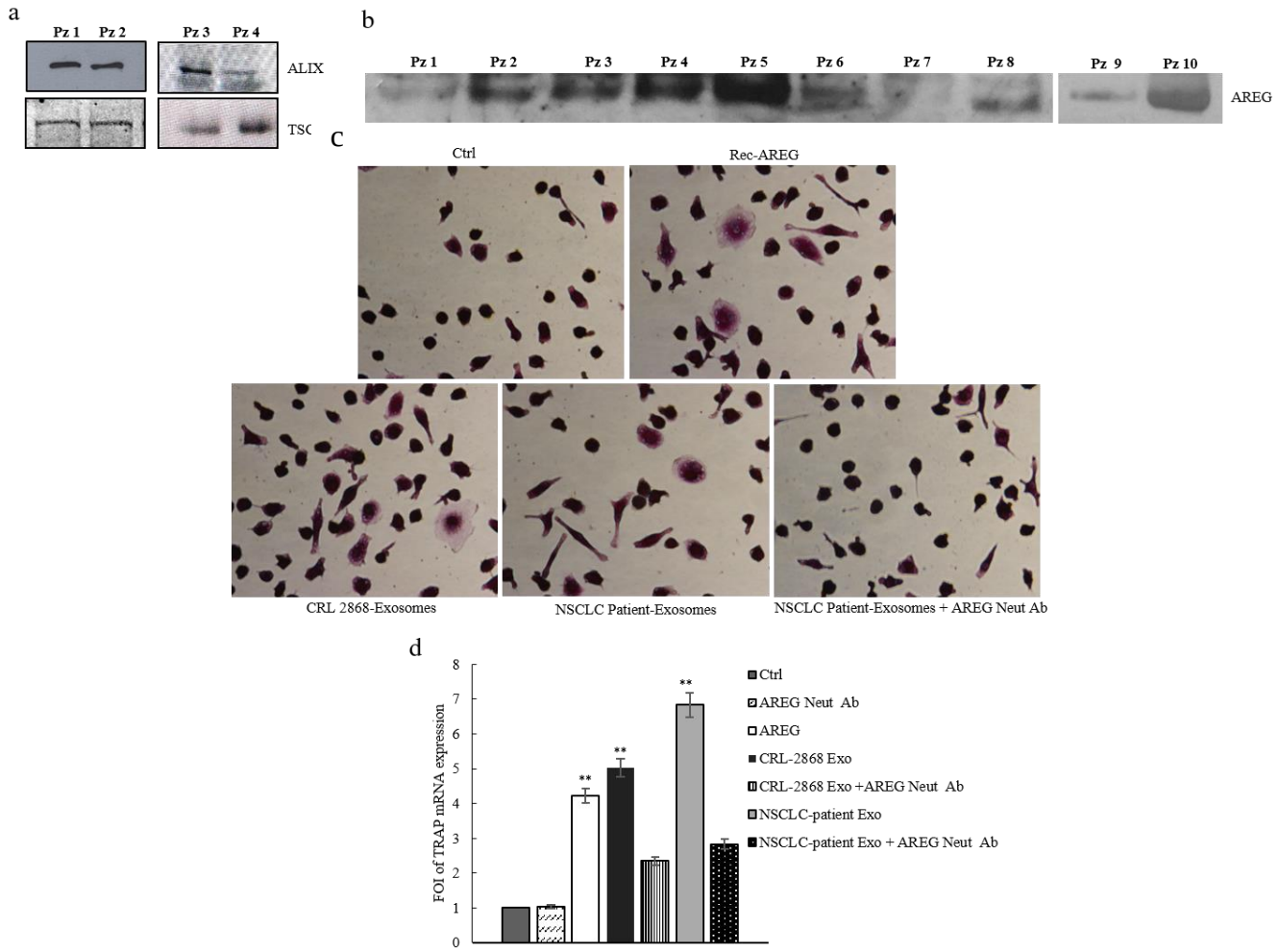

Figure 18: (**a**) Representative western blotting of ALIX and TSG 101 in 30 µg of exosomes isolated from plasma (1, 5 ml) of four NSCLC patients (Pz 1: stage I, Pz 2: stage IB, Pz 3: stage IIIA, Pz 4: stage IIIA). (**b**) Representative western blotting of AREG in 30 µg of exosomes isolated from plasma of ten NSCLC patients at different disease stages (Pz 1: stage I, Pz 2: stage IB, Pz 3: stage III, Pz 4: stage IIIA, Pz 5:stage IV, Pz 6:stage IV, Pz 7:stage IV, Pz 8:stage IV, Pz 9:stage IV, Pz 10:stage IV). (**c**) TRAP staining of human pOCs cultured in differentiation medium and incubated with: REC-AREG, CRL-2868 exosomes, NSCLC-patient exosomes, NSCLC-patient exosomes plus AREG neutralizing antibodies. Scale bar 10 µm. (**d**) Evaluation by Real Time PCR of TRAP mRNA expression, in primary human pre-osteoclasts, treated for 4 days, with: CRL-2868 exosomes, AREG neutralizing antibodies, NSCLC patient exosomes, CRL-2868 exosomes plus AREG neutralizing antibodies, NSCLC patients exosomes plus AREG neutralizing antibodies.

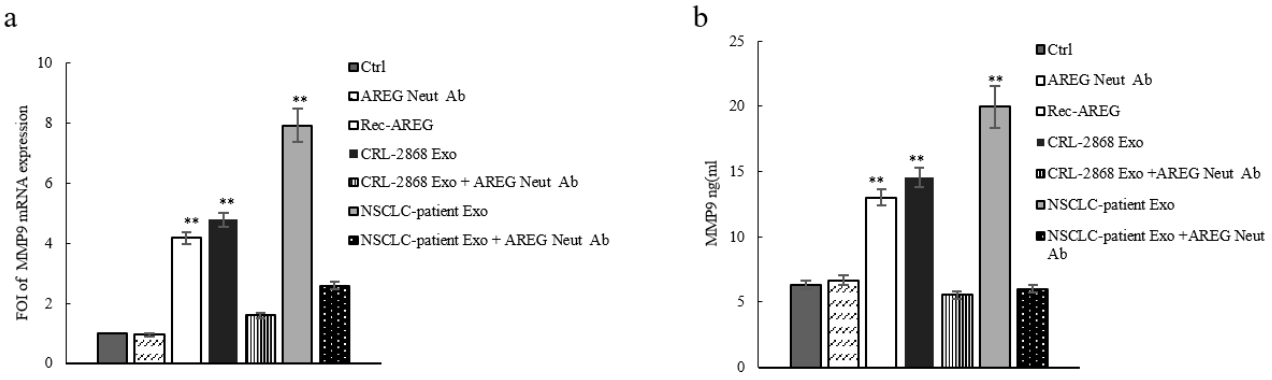

Figure 19: (a) MMP9 mRNA expression, in primary human pre-osteoclasts, treated for 4 days, with: CRL-2868 exosomes, AREG neutralizing antibodies, NSCLC patient exosomes, CRL-2868 exosomes plus AREG neutralizing antibodies, NSCLC patients exosomes plus AREG neutralizing antibodies. (**b**) MMP9 protein levels assessed by ELISA, in primary human pre-osteoclasts treated for 4 days with: CRL-2868 exosomes, AREG neutralizing antibodies, NSCLC patient exosomes, CRL-2868 exosomes plus AREG neutralizing antibodies, NSCLC patients exosomes plus AREG neutralizing antibodies.

Table 1

Primer sequences		
Gene	**Forward primer sequence (5'-3')**	**Reverse primer sequence (5'-3')**
mouse GAPDH	CCCAGAAGACTGTGGATGG	CAGATTGGGGGTAGGAACAC
mouse TRAP	GCGACCATTGTTAGCCACATACG	CGTTGATGTCGCACAGAGGGAT
mouse MMP9	GCTGACTACGATAAGGACGGCA	GCGGCCCTCAAAGATGAACGG
mouse RANKL	TCTCTGGGTCTAACCCCTGG	CAGGTCCCAGCGCAATGTAA
human GAPDH	ATGGGGAAGGTGAAGGTCG	GGGTCATTGATGGCAACAATATC
human TRAP	GATCCTGGGTGCAGACTTCA	GCGCTTGGAGATCTTTAGAGT
human MMP9	CGCTACCACCTCGAACTTTG	GCCATTCACGTCGTCCTTAT
human RANKL	AAGGCAGAATGTGTACCAGGG	CTTGCCTCTGGCTGGAAACC
human AREG	GTGGTGCTGTCGCTCTTGATACTC	TCAAATCCATCAGCACTGTGGTC

Bibliography

1. Howlader NNA, Noone AM, Krapcho M, Garshell J, Neyman N, Altekruse SF, et al. Lung Cancer. In SEER Cancer Statistics Review, 1975-2010. National Cancer Institute, Bethesda, MD.2013. *Internet Communication* (2013).
2. Siegelin MD, Borczuk AC. Epidermal growth factor receptor mutations in lung adenocarcinoma. *Lab Invest* 94 (2):129-37 (2014).
3. Jemal A., Siegel R., Ward E., Hao Y. Cancer statistics 2009. CA *Cancer J.Clinic*. 59, 225-249 (2009).
4. Perisano C., Spinelli MS, Graci C., Scaramuzzo L., Marzetti E., Barone C., Fabbriciani C., Maccauro G. Soft tissue metastases in lung cancer: a review of the literature. *Eur Rev Med* Pharmacol Sci 16, 1908–1914 (2012).
5. Tsuya A., Kurata T., Tamura K. & Fukuoka M. Skeletal metastases in non-small cell lung cancer: a retrospective study. *Lung Cancer* 57, 229–232 (2007).
6. Roato I, Gorassini E, Buffoni L, Lyberis P, Ruffini E, Bonello L, Baldi I, Ciuffreda L, Mussa A, Ferracini R. Spontaneous osteoclastogenesis is a predictive factor for bone metastases from non-small cell lung cancer. *Lung Cancer* 61 (1):109-16 (2008).
7. Miller R. E., Jones J. C., Tometsko M., Blake M. L. & Dougall, W. C. RANKL inhibition blocks osteolytic lesions and reduces skeletal tumor burden in models of non-small-cell lung cancer bone metastases. *J Thorac Oncol* 9, 345–354 (2014).
8. Riess J. W. & Wakelee H. A. Metastatic non-small cell lung cancer management: novel targets and recent clinical advances. *Clin Adv Hematol Oncol* 10, 226–234 (2012).
9. Dancey J, Sausville EA. Issues and progress with protein kinase inhibitors for cancer treatment. *Nat Rev Drug Discov* 1: 296–313 (2003).
10. Schneider M.R. and Wolf E. The epidermal growth factor receptor ligands at a glance. *J Cell. Physiol.* 218, 460-466 (2009).
11. Linggi B, Carpenter G. ErbB receptors: New insights on mechanisms and biology. *Trends Cell Biol.* 16:649–656 (2006).
12. M. J. Wieduwilt, M. M. Moasser. The epidermal growth factor receptor family: Biology driving targeted therapeutics. *Cell Mol Life Sci*. 65 (10): 1566–1584 (2008).

13. Schulze WX, Deng L, Mann M. Phosphotyrosine interactome of the ErbB-receptor kinase family. *Molecular systems biology* 1:2005.0008 (2005).

14. Zarich N, Oliva JL, Martinez N, Jorge R, Ballester A, Gutierrez-Eisman S, Garcia-Vargas S, Rojas JM. Grb2 is a negative modulator of the intrinsic Ras-GEF activity of hSos1. *Molecular Biology of the Cell*. 17 (8): 3591–7 (2006).

15. Avruch J, Khokhlatchev A, Kyriakis JM, et al. Ras activation of the Raf kinase: tyrosine kinase recruitment of the MAP kinase cascade. *Recent Progress in Hormone Research*. 56 (1): 127–55 (2001).

16. Liebmann C. Regulation of MAP kinase activity by peptide receptor signalling pathway: paradigms of multiplicity. *Cell Signal* 13: 777-785 (2001).

17. Jorissen RN, Walker F, Pouliot N et al. Epidermal growth factor receptor: mechanisms of activation and signalling. *Exp Cell Res* 284:31–53 (2003).

18. Guo Y, Du J, Kwiatkowski DJ. Molecular dissection of AKT activation in lung cancer cell lines. *Mol Cancer Res* 11:282-293 (2013).

19. Takata S, Takigawa N, Segawa T, et al. STAT3 expression in activating EGFR-driven adenocarcinoma of the lung. *Lung Cancer* 5:24-29 (2012).

20. Chan BA, Hughes BG. Targeted therapy for non-small cell lung cancer: current standards and the promise of the future. *Transl Lung Cancer Res*. 4:36–54 (2015).

21. Lynch TJ, Bell DW, Sordella R, et al. Activating mutations in the epidermal growth factor receptor underlying responsiveness of non-small-cell lung cancer to gefitinib. *N Engl J Med.* 350:2129–2139 (2004).

22. Pao W, Miller V, Zakowski M, et al. EGF receptor gene mutations are common in lung cancers from "never smokers" and are associated with sensitivity of tumors to gefitinib and erlotinib. *Proc Natl Acad Sci U S A*. 101:13306–13311 (2004).

23. Shepherd FA, Rodrigues PJ, Ciuleanu T, et al. Erlotinib in previously treated non-small-cell lung cancer. *N Engl J Med*. 353:123–132 (2005).

24. Thatcher N, Chang A, Parikh P, et al. Gefitinib plus best supportive care in previously treated patients with refractory advanced non-small-cell lung cancer: results from a randomised, placebo-controlled, multicentre study (Iressa Survival Evaluation in Lung Cancer) *Lancet*. 366:1527–1537 (2005).

25. AF Gazdar. Activating and resistance mutations of EGFR in non-small-cell lung cancer: role in clinical response to EGFR tyrosine kinase inhibitors *Oncogene* 28 Suppl 1: S24-31 (2009).

26. Ferguson K.M., Berger M.B., Mendrola J.M., Cho H.S., Leahy D.J., Lemmon M.A. EGF activates its receptor by removing interactions that autoinhibit ectodomain dimerization. *Moll. Cell* 11:507–517 (2003).

27. Cho H.S., Leahy D.J. Structure of the extracellular region of HER3 reveals an interdomain tether. *Science* 297:1330–1333 (2002).

28. Bouyain S., Longo P.A., Li S., Ferguson K.M., Leahy D.J. The extracellular region of ErbB4 adopts a tethered conformation in the absence of ligand. Proc. *Natl. Acad. Sci. USA*. 102:15024–15029 (2005).

29. Riely GJ, Politi KA, Miller VA, Pao W. Update on epidermal growth factor receptor mutations in non-small cell lung cancer. *Clin Cancer Res*. 12:7232–7241 (2006).

30. Chou TY, Chiu CH, Li LH *et al*. Mutation in the tyrosine kinase domain of epidermal growth factor receptor is a predictive and prognostic factor for gefitinib treatment in patients with non-small cell lung cancer. *Clin Cancer Res* 11:3750–3757 (2005).

31. Mitsudomi T, Kosaka T, Endoh H *et al*. Mutations of the epidermal growth factor receptor gene predict prolonged survival after gefitinib treatment in patients with non-small-cell lung cancer with postoperative recurrence. *J Clin Oncol* 23:2513–2520 (2005).

32. Yun, T.J. Boggon, Y. Li, M.S. Woo, H. Greulich, M. Meyerson, M.J. Eck. Structures of lung cancer-derived EGFR mutants and inhibitor complexes: mechanism of activation and insights into differential inhibitor sensitivity. *Cancer Cell* 11, pp. 217-227 (2007).

33. Carey KD, Garton AJ, Romero MS, Kahler J, Thomson S, Ross S, Park F, Haley JD, Gibson N, Sliwkowski MX. Kinetic analysis of epidermal growth factor receptor somatic mutant proteins shows increased sensitivity to the epidermal growth factor receptor tyrosine kinase inhibitor, erlotinib. *Cancer Res* 66, pp. 8163-8171 (2006).

34. Y. Shan, M.P. Eastwood, X. Zhang, E.T. Kim, A. Arkhipov, R.O. Dror, J. Jumper, J. Kuriyan, D.E. ShawOncogenic mutations counteract intrinsic disorder in the EGFR kinase and promote receptor dimerization. *Cell* 149 pp. 860-870 (2012).

35. Yun CH, Boggon TJ, Li Y, Woo MS, Greulich H, Meyerson M, Eck MJ. Structures of lung cancer-derived EGFR mutants and inhibitor complexes: Mechanism of activation and insights into differential inhibitor sensitivity. *Cancer Cell* 11:217–227 (2007).

36. Zhang X, Gureasko J, Shen K, Cole PA, Kuriyan J. An allosteric mechanism for activation of the kinase domain of epidermal growth factor receptor. *Cell* 125:1137–1149 (2006).

37. J. Stamos, M.X. Sliwkowski, C. Eigenbrot. Structure of the epidermal growth factor receptor kinase domain alone and in complex with a 4-anilinoquinazoline inhibitor *J. Biol. Chem* 277, pp. 46265-46272 (2002).

38. C.H. Yun, T.J. Boggon, Y. Li, M.S. Woo, H. Greulich, M. Meyerson, M.J. Eck Structures of lung cancer-derived EGFR mutants and inhibitor complexes: mechanism of activation and insights into differential inhibitor sensitivity *Cancer Cell* 11, pp. 217-227 (2007).

39. Ketan S. Gajiwala, Junli Feng, Rose Ann Ferre, Kevin Ryan, Oleg Brodsky Scott Weinrich John C. Kath AlStewart. Insights into the Aberrant Activity of Mutant EGFR Kinase Domain and Drug Recognition. *Structure* 5;21(2):209-19 (2013).

40. Sakurada A, Shepherd FA, Tsao MS. Epidermal growth factor receptor tyrosine kinase inhibitors in lung cancer: impact of primary or secondary mutations. *Clin Lung Cancer* 7 (Suppl 4): S138–S144 (2006).

41. Gil-Bazo I, Rolfo C. AZD9291 in TKI EGFR resistance in non-small cell lung cancer and the new concept of phase I trials. *Transl lung cancer Res* 5 (1):85-8 (2016).

42. George R., Blumenschein, Jr, Gordon B. Mills, and Ana M. Gonzalez-Angulo. Targeting the Hepatocyte Growth Factor–cMET Axis in Cancer Therapy. *J Clin Oncol*. 10;30 (26) :3287-96 (2012).

43. Engelman JA, Zejnullah K, Mitsudomi T, Song Y, Hyland C, Park JO, Lindeman N, Gale CM, Zhao X, Christensen J, Kosaka T, Holmes AJ, Rogers AM, Cappuzzo F, Mok T, Lee C, Johnson BE, Cantley LC, Janne PA. MET amplification leads to gefitinib resistance in lung cancer by activating ERBB3 signaling. *Science* 18;316(5827):1039-43 (2007).

44. Z Tang, R Du, S Jiang, C Wu, D S Barkauskas, J Richey, J Molter, M Lam, C Flask, S Gerson, A Dowlati, L Liu, Z Lee, B Halmos, Y Wang, J A Kern, P C Ma. Dual MET-EGFR combinatorial inhibition against T790M-EGFR-mediated erlotinib-resistant lung cancer. *Br J Cancer* 16; 99(6): 911–922 (2008).

45. Yu HA, Arcila ME, Rekhtma N, et al. Analysis of tumor specimens at the time of acquired resistance to EGFR-TKI therapy in 155 patients with EGFR-mutant lung cancers. *Clin Cancer Res* 19:2240-2247 (2013).

46. Pao W, Wang TY, Riely GJ, Miller VA, Pan Q, Ladanyi M, Zakowski MF, Heelan RT, Kris MG, Varmus HE. *KRAS* mutations and primary resistance of lung adenocarcinomas to gefitinib or erlotinib. *PLoS Med* 2:57–61 (2005).

47. Antonio Marchetti, Michele Milella, Lara Felicioni, Federico Cappuzzo, Luciana Irtelli, Maela Del Grammastro, Mariagrazia Sciarrotta, Sara Malatesta, Carmen Nuzzo, Giovanna Finocchiaro, Bruno Perrucci, Donatella Carlone, Alain J Gelibter, Anna Ceribelli, Andrea Mezzetti, Stefano Iacobelli, Francesco Cognetti, and Fiamma Buttitta. Clinical Implications of *KRAS* Mutations in Lung Cancer Patients Treated with Tyrosine Kinase Inhibitors: An Important Role for Mutations in Minor Clones. *Neoplasia* 11(10): 1084–1092 (2009).

48. Sacha I. Rothschild, Oòiver Gautschi. Crizotinib in the Treatment of Non Small-Cell Lung Cancer. *Clinical Lung Cancer* 14 (5):473-80 (2013).

49. Sweis RF, Thomas S, Bank B, Fishkin P, Mooney C, Salgia R. Concurrent EGFR Mutation and ALK Translocation in Non-Small Cell Lung Cancer. *Cureus* 26;8(2): e513 (2016).

50. Soda M, Choi YL, Enomoto M, et al. Identification of the transforming EML4-ALK fusion gene in non-small-cell lung cancer. *Nature* 2;448(7153): 561-6 (2007).

51. Takaaki Sasaki, Scott J. Rodig, Lucian R. Chirieac, and Pasi A Janne. The Biology and Treatment of *EML4-ALK* Non-Small Cell Lung Cancer. *European Journal of cancer* 46 (10):1773-80 (2010).

52. Camidge DR, Bang YL, Kwak EL, et al. Activity and safety of crizotinib in patients with ALK positive non-small-cell lung cancer: updated results from a phase I study. *Lancet Oncol* 13(10): 1011-9 (2012).

53. Yoshino I, Yohena T, Kitaijima M, Ushijima C, Nishioka K, et al. Survival of non-small cell lung cancer patients with postoperative recurrence at distant organs. *Ann Thorac Cardiovasc Surg* 7: 204-209 (2001).

54. Brown JE, Cook RJ, Major P, Lipton A, Saad F, et al. Bone turnover markers as predictors of skeletal complications in prostate cancer, lung cancer, and other solid tumors. *J Natl Cancer Inst* 97: 59-69 (2005).

55. Coleman RE. Metastatic bone disease: clinical features, pathophysiology and treatment strategies. *Cancer Treat Rev* 27: 165-176 (2001).

56. Motyl KJ, Guntur AR, Carvalho AL, Rosen CJ. Energy metabolism of bone. *Toxic Pathol*. 1:192623317737065 (2017).

57. Novack DV, Mbalaviele G. Osteoclasts-Key Players in Skeletal Health and Disease. *Microbiol Spectr* 4(3) Review (2016).

58. Blair HC, Teitelbaum SL, Ghiselli R, Gluck S. Osteoclastic bone resorption by a polarized vacuolar proton pump. *Science* 245: 855-857 (1989).

59. Tanaka H, Tanabe N, Kawato T, Nakai K, Kariya T, Matsumoto S, Zhao N, Motohashi M, Maeno M. Nicotine affects bone resorption and suppresses the expression of cathepsin K, MMP-9 and vacuolar-type H (+)-ATPase d2 and actin organization in osteoclasts. *PLoS One* 8(3): e59402 (2013).

60. Simonet WS, Lacey DL, Dunstan CR, Kelley M, Chang MS, et al. Osteoprotegerin: a novel secreted protein involved in the regulation of bone density. *Cell* 89: 309-319 (1997).

61. Boyce BF, Xing L. Functions of RANKL/RANK/OPG in bone modeling and remodeling. *Arch Biochem Biophys* 473: 139-146 (2008).

62. Roodman GD. Mechanisms of bone metastasis. *Discov Med* 4:144-148 (2004).

63. Peng X, Guo W, Ren T, Lou Z, Lu X, Zhang S, Lu Q, Sun Y. Differential expression of the RANKL/RANK/OPG system is associated with bone metastasis in human non-small cell lung cancer. *PLoS One* 8:e58361 (2013).

64. Karapanagiotou EM, Terpos E, Dilana KD, Alamara C, Gkiozos I, et al. Serum bone turnover markers may be involved in the metastatic potential of lung cancer patients. *Med Oncol* 27: 332-338 (2010).

65. Di Lorenzo, G, Tortora G, D'Armiento FP, De Rosa G, Staibano S, Autorino R, D'Armiento M, De Laurentiis M, De Placido S, Catalano G, Bianco AR, Ciardiello F et al. Expression of epidermal growth factor receptor correlates with disease relapse and progression to androgen-independence in human prostate cancer. *Clin. Cancer Res* 8, 3438-3444 (2002).

66. Choueiri, M.B. et al. The cantral role of osteoblasts in the metastasis of prostate cancer. *Cancer Metastasis Rev* 25, 601-6019 (2006).

67. Buijs, J.T. and van dr Pluijm, G. Osteotropic cancers: from primary tumor to bone. *Cancer Lett* 273, 177-193 (2009).

68. Xian, C.J. Roles of epidermal growth factor family in the regulation of postnatal somatic growth. *Endocr. Rev.* 28, 284-296 (2007).

69. Zhu J, Jia X, Xiao G, Kang Y, Partridge NC, Qin L. EGF-like ligands stimulate osteoclastogenesis by regulating expression of osteoclast regulatory factors by osteoblasts, implications for osteolytic bone metastases *J. Biol. Chem.* 14; 282(37):26656-64 (2007).

70. M.S. Kim, Chris J. Day, Christine I. Selinger, Carly L. Magno, Sebastien R. J . Stephens, Nigol A.Morrison. MCP-1-induced human osteoclast-like cells are tartrate-resistant acid phosphatase, NFATc1, and Calcitonin Receptor-positive but Require Receptor Activator of NFκB Ligand for Bone Resorption. *J. Biol. Chem* 281, pp. 1274-1285 (2006).

71. E. Canalis, L.G. Raisz. Effect of epidermal growth factor on bone formation in vitro *Endocrinology* 104, pp. 862-869 (1979).

72. M. Kumegawa, M. Hiramatsu, K. Hatekeyama, T.Yajima, H.Kodama, T.Osaki, K.Kurisu. Effects of epidermal growth factor on osteoblastic cells in vitro *Calcif. Tissue Int* 35, pp. 542-548 (1983).

73. K.W. Ng, N.C. Partridge, M. Niall, T.J. Martin.Stimulation of DNA synthesis by epidermal growth factor in osteoblast-like cells *Calcif. Tissue Int* 35, pp. 624-628R (1983).

74. Ryu-Ichiro, Hisae Hori, Yutaka Nagai, Shigeyasu Tanaka, Mayuri Kondo, Masahiko Hiramatsu, Nobuo Utsumi, Masa Yoshi Kumegawa. Selective inhibition of type I collagen synthesis in osteoblastic cells by epidermal growth factor. Endocrinology 115, pp. 867-876 (1984).

75. M.A. Fang, D A Kujubu and T J Hahn. The effects of prostaglandin E2, parathyroid hormone, and epidermal growth factor on mitogenesis, signaling, and primary response genes in UMR 106-01 osteoblast-like cells *Endocrinology* 131, pp. 2113-2119 (1992).

76. J. Loza, L.Carpio, G. Lawless , N. Marzec, R. Dziak. Role of extracellular calcium influx in EGF-induced osteoblastic cell proliferation. *Bone,* 16, pp. 341S-347S (1995).

77. H.-H. Chien, W.-L Lin, M.-Il Cho. Down-regulation of osteoblastic cell differentiation by epidermal growth factor receptor Calcif. Tissue Int 67, pp. 141-150 (2000).

78. L. Qin, Tamasi J, Raggatt L, Li X, Feyen JH, Lee DC, Amphiregulin is a novel growth factor involved in normal bone development and in the cellular response to parathyroid hormone stimulation *J. Biol. Chem* 280, pp. 3974-3981 (2005).

79. Gschwind, A., Oliver M, Fischer Axel Ulrich. The discovery of receptor tyrosine kinases: targets for cancer therapy. *Nat. Rev. Cancer* 4, 361-370 (2004).

80. Monsonego, E., Orna Halevy, Arieh Gerther, Shmuel Hurwitz, Mark Pines. Growth hormone inhibits differentiation of avian epiphyseal growth-plate chondrocytes. *Mol. Cell. Endocrinol*. 114, 35-42 (1995).

81. L.G. Raisz, Simmons HA, Sandberg AL, Canalis E. Direct stimulation of bone resorption by epidermal growth factor Endocrinology, 107, pp. 270-273 (1980).

82. Stern PH, Krieger NS, Nissenson RA, Williams RD, Winkler ME, Derynck R, Strewler GJ. Human transforming growth factor-alpha stimulates bone resorption in vitro *J. Clin. Invest,* 76, pp. 2016-2019 (1985).

83. K.J. Ibbotson, *et al.* Human recombinant transforming growth factor alpha stimulates bone resorption and inhibits formation in vitro Proc. *Natl. Acad. Sci. U. S. A.*, 83, pp. 2228-2232 (1986).

84. J.A. Lorenzo, Quinton J, Sousa S, Raisz LG. Effects of DNA and prostaglandin synthesis inhibitors on the stimulation of bone resorption by epidermal growth factor in fetal rat long-bone cultures *J. Clin. Invest*., 77, pp. 1897-1902 (1986).

85. N. Takahashi, Mac Donald BR, Hon J, Winkler ME, Derynch R, Mundy GR, Roodman GD. Recombinant human transforming growth factor-alpha stimulates the formation of osteoclast-like cells in long-term human marrow cultures *J. Clin. Invest*., 78, pp. 894-898 (1986).

86. A.H. Tashjian Jr., E F Voelkel, W Lloyd, R Derynck, M E Winkler, L Levine. Actions of growth factors on plasma calcium. Epidermal growth factor and human transforming growth factor-alpha cause elevation of plasma calcium in mice *J. Clin. Invest.,* 78, pp. 1405-1409 (1986).

87. P.J. Marie, *et al.* Effects of epidermal growth factor on bone formation and resorption in vivo. *Am. J. Physiol*., 258, pp. E275-E281 (1990).

88. Tkach M, Thery C. Communication by Extracellular Vesicles: Where We Are and Where We Need to Go. Cell. p. 1226–32 (2016).

89. Raposo G, Stoorvogel W. Extracellular vesicles: Exosomes, microvesicles, and friends. *J. Cell Biol.* p. 373–83 (2013).

90. Johnstone RM, Adam M, Hammond JR, Orr L, Turbide C. Vesicle formation during reticulocyte maturation. Association of plasma membrane activities with released vesicles (exosomes*). J Biol Chem* 262: 9412-20 (1987).

91. Schmidt O, Teis D. The ESCRT machinery. *Curr Biol* 22:116-20 (2012).

92. Katzmann DJ, Babst M, Emr SD. Ubiquitin-dependent sorting into the multivescicular body pathway requires the function of a conserved endosomal protein sorting complex, ESCRT-1. *Cell* 106:145-55 (2001).

93. Wollert T, Wunder C, Lippincott-Schwartz J, Hurley JH. Membranee sciccion by the ESCRT-III complex. *Nature* 458: 172-7 (2009).

94. Kowal J, Tkach M, Théry C. Biogenesis and secretion of exosomes. *Curr Opin Cell Bio*. 29:116–25 (2014).

95. Fader CM, Sanchez DG, Mestre MB, Colombo MI. TI-VAMP/VAMP7 and VAMP3/cellubrevin: two v-SNARE proteins involved in specific steps of the autophagy/multivesicular body pathways. *Biochim Biophys Acta*. 1793(12):1901–16 (2009).

96. Rao SK, Huynh C, Proux-Gillardeaux V, Galli T, Andrews NW. Identification of SNAREs involved in synaptotagmin VII-regulated lysosomal exocytosis. *J Biol Chem.* 279(19):20471–9 (2004).

97. Trajkovic K, Hsu C, Chiantia S et al. Ceramide triggers budding of exosome vesicles into multivescicular endosomes. *Science* 319:1244-7 (2008).

98. Bobrie A, Colombo M, Raposo G, Thery C. Exosome secretion: molecular mechanisms and roles in immune responses. *Traffic* 12:1659-68 (2011).

99. Chow A, Zhou W, Liu L, Fong MY, Champer J, Van Haute D, et al. Macrophage immunomodulation by breast cancer-derived exosomes requires Toll-like receptor 2-mediated activation of NF-kappaB. *Sci Rep* 4:5750 (2014).

100. Costa-Silva B, Aiello NM, Ocean AJ, Singh S, Zhang H, Thakur BK, et al. Pancreatic cancer exosomes initiate pre-metastatic niche formation in the liver. *Nat Cell Biol* 17(6):816–26 (2015).

101. Raimondo S, Saieva L, Corrado C, Fontana S, Flugy A, Rizzo A, et al. Chronic myeloid leukemia-derived exosomes promote tumor growth through an autocrine mechanism. *Cell Commun Signal* 3; 13:8 (2015).

102. Hupfeld T, Chapuy B, Schrader V, Beutler M, Veltkamp C, Koch R, et al. Tyrosine kinase inhibition facilitates cooperation of transcription factor SALL4 and ABC transporter A3 towards intrinsic CML cell drug resistance. *Br J Haematol* 161 (2):204–13 (2013).

103. Safaei R, Larson BJ, Cheng TC, Gibson MA, Otani S, Naerdemann W, et al. Abnormal lysosomal trafficking and enhanced exosomal export of cisplatin in drug-resistant human ovarian carcinoma cells. *Mol Cancer Ther* 4(10):1595–604 (2005).

104. Langley RR and Fidler IJ: Tumor cell-organ microenvironment interactions in the pathogenesis of cancer metastases. *Endocr Reviews* 28: 297-321 (2007).

105. Langley RR and Fidler IJ: The seed and soil hypothesis revisited – the role of tumor-stroma interactions in metastasis to different organs. *Int J Cancer* 128: 2527-2535 (2011).

106. Vanharanta S and Massague J: Origins of metastatic traits. *Cancer Cell* 24: 410-421 (2013).

107. Weidle UH, Birzele F, Kollmorgen G, Ruger R. The Multiple Roles of Exosomes in Metastasis. *Cancer Genomics Proteomics*. 2;14(1):1-15 (2017).

108. Massague J and Obenauf AC: Metastatic colonization by circulating tumor cells. *Nature* 529: 298-306 (2016).

109. Chiang AC, Massague: Molecular basis of metastasis. *N Engl J Med* 359: 2814-2823 (2008).

110. Nguyen DX, Bos PD, Massague J: Metastasis: from dissemination to organ-specific colonization. *Nat Rev Cancer* 9: 274-284 (2009).

111. Paget S: The distribution of secondary growths in cancer of the breast. *Cancer Metastasis Rev* 8: 98-101 (1989)

112. Al-Nedawi K, Meehan B, Kerbel RS, Allison AC, Rak J. Endothelial expression of autocrine VEGF upon the uptake of tumor-derived microvescicles containing oncogenic EGFR. *Proc Natl Acad Sci U S A*. 10;106 (10):3794-9 (2009).

113. Peinado H, Alečković M, Lavotshkin S, Matei I, Costa-Silva B, Moreno-Bueno G, Hergueta-Redondo M, Williams C, García-Santos G, Ghajar C, Nitadori-Hoshino A, Hoffman C, Badal K, Garcia BA, Callahan MK, Yuan J, Martins VR, Skog J, Kaplan RN, Brady MS, Wolchok JD, Chapman PB, Kang Y, Bromberg J, Lyden D. Melanoma exosomes educate bone marrow progenitor cells toward a pro-metastatic phenotype through MET. *Nat Med*. 18(6):883-91 (2012).

114. Raimondi L, De Luca A, Amodio N, Manno N, Raccosta S, Taverna S, Bellavia D, Naselli F, Fontana S, Schillaci O, Giardino R, Fini M, Tassone P, Santoro A, De Leo G, Giavaresi G, Alessandro R. Involvement of multiple myeloma cell-derived exosomes in osteoclast differentiation. *Oncotarget* 30;6(15):13772-89 (2015).

115. Jung T, Castellana D, Klingbeil P, Cuesta Hernandez I, Vitacolonna M, Orlicky DJ, Roffler SR, Brodt P, Zöller M: CD44v6 dependance of premetastatic niche preparation by exosomes. *Neoplasia* 11: 1093-1105 (2009).

116. Werbowetski-Ogilvie TE, Bhatia M. Pluripotent human stem cell lines: what we can learn about cancer initiation. *Trends Mol Med*. 14:323–332 (2008).

117. Bidard FC, Pierga JY, Vincent-Salomon A, Poupon MF. A "class action" against the microenvironment: do cancer cells cooperate in metastasis? *Cancer Metastasis Rev*. 27:5–10 (2008).

118. Ponta H, Sherman L, Herrlich PA. CD44: from adhesion molecules to signalling regulators. *Nat Rev Mol Cell Biol*. 4:33–45 (2003).

119. Toole BP, Slomiany MG. Hyaluronan, CD44 and Emmprin: partners in cancer cell chemoresistance. *Drug Resist Updat*. 11:110–121 (2008).

120. James N. Higginbotham, Michelle Demory Beckler, Jonathan D. Gephart, Jeffrey L. Franklin, Galina Bogatcheva, Gert-Jan Kremers, David W. Piston, Gregory D. Ayers, Russell E. McConnell, Matthew J. Tyska, Robert J. Coffey. Amphiregulin exosomes increase cancer cell invasion. *Curr Biol.* 21(9): 779–786 (2011).

121. Corrado C, Saieva L, Raimondo S, Santoro A, De Leo G, Alessandro R. Chronic myelogenous leukaemia exosomes modulate bone marrow microenvironment through activation of epidermal growth factor receptor. *J Cell Mol Med.* 20(10):1829-39 (2016).

122. Yi T, et al. Epidermal growth factor receptor regulates osteoclast differentiation and survival through cross-talking with RANK signaling. *J Cell Physiol*. 217:409–422 (2008).

123. Chang MH, et al. Clinical impact of amphiregulin expression in patients with epidermal growth factor receptor (EGFR) wild-type nonsmall cell lung cancer treated with EGFR-tyrosine kinase inhibitors. *Cancer.* 117:143–151 (2011).

124. Rolfo C, Giallombardo M, Reclusa P, Sirera R, Peeters M. Exosomes in lung cancer liquid biopsies: Two sides of the same coin? *Lung Cancer.* 10-1 (2016).

125. Passiglia F, Pauwels P, Rolfo C, et al. The role of cMET in non-small cell lung cancer resistant to EGFR-inhibitors: did we really find the target? *CurrDrugTargets.*15(14):1284-92 (2014).

126. Pérez-Ramírez C, Cañadas-Garre M, Robles AI, Molina MÁ, Faus-Dáder MJ, Calleja-Hernández MÁ. Liquid biopsy in early stage lung cancer. *Transl Lung Cancer Res*. 5(5):517-524 Review (2016).

127. Pérez-Callejo D, Romero A, Provencio M, Torrente M. Liquid biopsy based biomarkers in non-small cell lung cancer for diagnosis and tretament monitoring. *Transl Lung Cancer Res.* 5(5):455-465. Review (2016).

128. Jin X, Chen Y, Chen H, Fei S, Chen D, Cai X, Liu L, Lin B, Su H, Zhao L, Su M, Pan H, Shen L, Xie D, Xie C. Evaluation of Tumor-Derived Exosomal miRNA as Potential Diagnostic Biomarkers for Early-Stage Non-Small Cell Lung Cancer Using Next-Generation Sequencing. *Clin Cancer Res*. 23(17):5311-5319 (2017).

129. Liu Q, Yu Z, Yuan S, Xie W, Li C, Hu Z, Xiang Y, Wu N, Wu L, Bai L, Li Y. Circulating exosomal microRNAs as prognostic biomarkers for non-small-cell-lung cancer. *Oncotarget.* 21;8(8):13048-13058 (2017).

130. Sandfeld-Paulsen B, Aggerholm-Pedersen N, Bæk R, Jakobsen KR, Meldgaard P, Folkersen BH, Rasmussen TR, Varming K, Jørgensen MM, Sorensen BS. Exosomal proteins as prognostic biomarkers in non-small cell lung cancer. *Mol Oncol.* 10(10):1595-1602 (2016).

131. Cordonnier M, Chanteloup G, Isambert N, Seigneuric R, Fumoleau P, Garrido C, et al. Exosomes in cancer theranostic: Diamonds in the rough. *Cell Adh Migr*. 1–13 (2017).

132. Boukouris S, Mathivanan S. Exosomes in bodily fluids are a highly stable resource of disease biomarkers. *Proteomics Clin Appl*. 9 (3-4):358-67 (2015).

133. Maas S, Breakefield X, Weaver A. Extracellular Vesicles: Unique Intercellular Delivery Vehicles. *Trends Cell Biol*. S0962-8924:30179–9 (2016).

134. Hannafon BN, Ding W-Q. Intracellular communication by exosome- derived microRNAs in cancer. *Int J Mol Sci* 14:14240 (2013).

135. Ge R, Tan E, Sharghi-Namini S, Asada HH. Exosomes in cancer microenvironment and beyond: have we overlooked these extracel- lular messengers? *Cancer Microenviron* 5:323 (2012).

136. Hu G, Drescher KM, Chen X-M. Exosomal miRNAs: biological properties and therapeutic potential. Front Genet 3:56 (2012).

137. Gallo A, Tandon M, Alevizos I, Illei GG. The majority of microRNAs detectable in serum and saliva is concentrated in exosomes. *PLoS One.* 7(3): e30679 (2012).

138. Rabinowits G, Gercel-Taylor C, Day JM, Taylor DD, Kloecker GH. Exosomal microRNA: a diagnostic marker for lung cancer. *Clin Lung Cancer* 10:42-6.10.3816/CLC.2009.n.006 (2009).

139. Cazzoli, R. et al. microRNAs derived from circulating exosomes as noninvasive biomarkers for screening and diagnosis lung cancer. *J. Thorac. Oncol*. 8, 1156-1162 (2013).

140. Yuwen D-L, Sheng B-B, Liu J, Wenyu W, Shu Y-Q. miR-146a-5p level in serum exosomes predicts therapeutic effect of cisplatin in non-small cell lung cancer. *Eur Rev Med Pharmacol* Sci. 21(11):2650-8 (2017)

141. Yuan D, Xu J, Wang J, Pan Y, Fu J, Bai Y, et al. Extracellular miR-1246 promotes lung cancer cell proliferation and enhances radioresistance by directly targeting DR5. *Oncotarget.* (2016).

142. Tang Y, Cui Y, Li Z, Jiao Z, Zhang Y, He Y, et al. Radiation-induced miR-208a increases the proliferation and radioresistance by targeting p21 in human lung cancer cells. *L Exp Clin Cancer Res.* 35:7 (2016).

143. Rolfo C, Laes JF, Reclusa P, Valentino A, Lienard M, Gil-Balzo I, et al. P2.01-093 Exo-ALK Proof of Concept: Exosomal Analysis of ALK Alterations in Advanced NSCLC Patients. *J Thorac Oncol.* 14; 12 (1): S844-5 (2017).

144. J.O. Park, *et al.*Identification and characterization of proteins isolated from microvesicles derived from human lung cancer pleural effusions. *Proteomics,* 13 pp. 2125-2134 (2013).

145. Y. Li, *et al.*Proteomic identification of exosomal LRG1: a potential urinary biomarker for detecting NSCLC . *Electrophoresis*, 32 pp. 1976-1983 (2011).

146. T. Yamashita, *et al.*Epidermal growth factor receptor localized to exosome membranes as a possible biomarker for lung cancer diagnosis *Die Pharmazie*, 68 pp. 969-973 (2013).

147. S.H. Huang, *et al.*Epidermal growth factor receptor-containing exosomes induce tumor-specific regulatory T cells *Cancer Invest*., 31, pp. 330-335 (2013).

148. K. Ueda, *et al.*Antibody-coupled monolithic silica microtips for highthroughput molecular profiling of circulating exosomes *Sci. Rep*., 4, p. 6232 (2014).

149. B. Sandfeld-Paulsen, N. Aggerholm-Pedersen, R. Bæk, K.R. Jakobsen, P. Meldgaard, B.H. Folkersen, T.R. Rasmussen, K. Varming, M.M. Jørgensen, B.S. Sorensen. Exosomal proteins as prognostic biomarkers in non small cell lung cancer. *Mol Oncol*. 10(10): 1595–1602 (2016).

150. Whiteside TL. Tumor-Derived Exosomes and Their Role in Tumor-Induced Immune Suppression. *Vaccines*. 4(4) (2016).

151. Jakobsen KR, Paulsen BS, Baek R, Varming K, Sorensen BS, Jorgensen MM. Exosomal proteins as potential diagnostic markers in advanced non-small cell lung carcinoma. J Extracell vescicles. 4:26659 (2015)

152. Théry C, Amigorena S, Raposo G, Clayton A. Isolation and characterization of exosomes from cell culture supernatansts and biological fluids. *Curr Protoc Cell Biol*. Chapter 3: Unit 3.22 (2006).

153. Riess JW, Wakelee HA. Metastatic non-small cell lung cancer management: novel targets and recent clinical advances. *Clin Adv Hematol Oncol*.10:226–234 (2012).

154. Kasahara K, et al. Impact of serum hepatocyte growth factor on treatment response to epidermal growth factor receptor tyrosine kinase inhibitors in patients with non-small cell lung adenocarcinoma. *Clin Cancer Res*. 16:4616–4624 (2010).

155. Owen, S., Ye, L., Sanders, A. J., Mason, M. D. & Jiang, W. G. Expression profile of receptor activator of nuclear-kappaB (RANK), RANK ligand (RANKL) and osteoprotegerin (OPG) in breast cancer. *Anticancer Res* 33, 199–206 (2013).

156. Guise, T. A. *et al*. Basic mechanisms responsible for osteolytic and osteoblastic bone metastases. *Clin Cancer Res* 12, 6213s–6216s (2006).

157. Wang K, Yamamoto H, Chin JR, Werb Z, Vu TH. Epidermal growth factor receptor-deficient mice have delayed primary endochondral ossification because of defective osteoclast recruitment. *J Biol Chem* (2004).

Scientific Products: publications, book chapters and acts in congresses

Publications:

- **Discussed in this thesis:**

- **Amphiregulin container in NSCLC-exosomes induces osteoclast differentiation through the activation of EGFR pathway**. Taverna S, Pucci M, Giallombardo M, Di Bella MA, Santarpia M, Reclusa P, Gil-Bazo I, Rolfo C, Alessandro R. Sci Rep. 2017 Jun 9;7(1):3170. doi: 10.1038/s41598-017-03460-y.

- **Not included in this thesis:**

- **Curcumin modulates Chronic Myelogenous Leukemia exosomes composition and affects angiogenic phenotype, via exosomal miR-21.** Simona Taverna, Simona Fontana, Francesca Monteleone, Marzia Pucci, Laura Saieva, Viviana De Caro, Valeria Giunta Cardinale, Marco Giallombardo, Christian Rolfo and Riccardo Alessandro. Oncotarget, 2016 Mar 30.

- **Curcumin inhibits in vitro and in vivo chronic myelogenous leukemia cells growth: a possible role for exosomal disposal of miR-21.** Taverna S, Giallombardo M, Pucci M, Flugy A, Manno M, Raccosta S, Rolfo C, De Leo G, Alessandro R. Oncotarget 2015 Jun 8.

- **Exosomes in Semen: opportunities as a new tool in cancer diagnosis.** M.Pucci*,S.Taverna*, P.Reclusa, Joseph A.Pinto, E.Durendez, Elosia Jantus Lewintre, M.Malarani, Giovanni Zito, C.Rolfo ,*Transl Cancer Res* 2017.

- **Exosomes as diagnostic biomarkers in lung cancer.** Pablo Reclusa*, Simona Taverna*, Marzia Pucci, Elena Durandez, Silvia Calabuig, Paolo Manca, Maria Jose Serrano, Laure Sober, Patrick Pauwels, Antonio Russo, Christian Rolfo. Review *J Thorac Dis* 2017.

- **Extracellular vesicles: small bricks for tissue repair/regeneration.** Taverna S, Pucci M, Alessandro R. Ann Transl Med. 2017 Feb;5(4):83. doi: 10.21037/atm.2017.01.53.

- **Exosomes as miRNA nano-shuttle: dual role in tumor progression.** Pucci Marzia, Pablo Reculsa Asiain, Elena Durendez Saez, Eloisa Jantus-Lewintre, Mahafarin Malarani, Shahanavaj Khan, Simona Fontana, Aung Naing, Christian Rolfo and Taverna Simona. Targeted Oncology. Under revision.

Acts in congresses

- POSTER SESSION (37TH EORTC PAMM WINTER MEETING IN ANTWERP, BELGIUM ON FEBRUARY 10-12, 2016 "IMPROVING TRANSLATIONAL REASEARCH FROM LAB TO CLINICAL PRACTICE". Effects of exosomes released by NSCLC cells on osteoclasts differentiation. Pucci M., Taverna S., Corrado C., Giallombardo M., Rolfo C. and Alessandro R.

- AWARD FOR BEST POSTER AT THE MEETING: "EXOSOMES IN PATHOLOGICAL CONDITIONS: NEW INSIGHTS FOR BIOMARKER DEVELOPMENT AND THERAPEUTIC APPLICATIONS", 9-10 GIUGNO, 2016. ISTITUTO SUPERIORE DI SANITA', ROMA AICC. Effects of exosomes released by NSCLC cells on osteoclasts differentiation. Pucci M., Taverna S., Corrado C., Giallombardo M., Rolfo C. and Alessandro R.

- IASLC 18TH WORLD CONFERENCE. Exosomal Amphiregulin induce osteoclastogenesis through osteoclast differentiation mediated by EGFR pathway in NSCLC. Christian Rolfo, Simona Taverna, Marzia Pucci, Maria Antonietta Di Bella, Pablo Reclusa, Gil-Bazo I, Riccardo Alessandro.

- MULTINATIONAL CONGRESS ON MICROSCOPY (SEPTEMBER 24-29, 2017 ROVINJ, CROATIA). ORAL PRESENTATION (Dott.ssa Maria Antonietta Di Bella). Role of NSCLC exosomes in osteoclast differentiation. Simona Taverna, Maria Antonietta Di Bella, Marzia Pucci, Marco Giallombardo, Christian Rolfo, Riccardo Alessandro.

- POSTER PRESENTATION EARC-AACR-SIC SPECIAL CONFERENCE 2017: THE CHALLENGE OF OPTIMISING IMMUNO AND TARGETED THERAPIES: FROM CANCER BIOLOGY TO THE CLINIC. Florence, 24-27 June 2017. Amphiregulin

contained in NSCLC exosomes induces osteoclast differentiation through the activation of EGFR pathway.

- AIBG CONGRESS, ORAL PRESENATION (Dott.ssa Simona Taverna) Cagliari, 30-09-2016. Effects of exosomes released by NSCLC cells on osteoclasts differentiation.

- POSTER SESSION XII-EVS IN CANCER (ISEV 2015): Curcumin induces selective packaging of miR-21 in exosomes released by chronic myelogenous leukaemia cells. Simona Taverna, Marco Giallombardo, Anna Flugy, Christian Rolfo, Marzia Pucci, Giacomo De Leo and Riccardo Alessandro.

- POSTER SESSION ITPA XI ANNUAL CONGRESS OF THE ITALIAN PROTEOMICS ASSOCIATION, (PERUGIA, MAY, 16-19, 2016). Curcumin modulates chronic myelogenous leukemia exosomes composition and affects angiogenic phenotype, via exosomal miR-21. Taverna S, Fontana S, Monteleone F, Pucci M, Saieva L, De Caro V, Cardinale VG, Giallombardo M, Vicario E, Rolfo C, De Leo G, Alessandro R.

Acknowledgements

I would like to thank all those who have accompanied me during the training process:

- A special thanks is addressed to my tutor Prof Riccardo Alessandro, for giving me this opportunity to work on cancer research, i will always be grateful to him for his human and scientific support which he has always shown me.

- I would like to thanks also Drs. Simona Taverna, for supporting me in every technical and scientific step.

- A thanks also to all the Biology Section of the Biopathology and Medical Biotechnology Department (DIBIMED) at the University of Palermo, for being not only colleagues but also a family.

- A special thanks is addressed also to Prof. Christian Rolfo which, together with Prof. Marc Peeters, contributed to my scientific and personal growth.

Finally, I thank all my family for believed in me and supported me during all my PhD training experience.